PET, TOFPET & SPECT

Chin-Tu Chen

Chien-Min Kao, Christian Wietholt, Qingguo Xie, Yun Dong, Jeffrey Souris, Hsing-Tsuen Chen, Bill C. O'Brien-Penney, Patrick J. La Riviere, Xiaochuan Pan

Department of Radiology & Committee on Medical Physics

Pritzker School of Medicine & Division of Biological Sciences

The University of Chicago

PET Principle

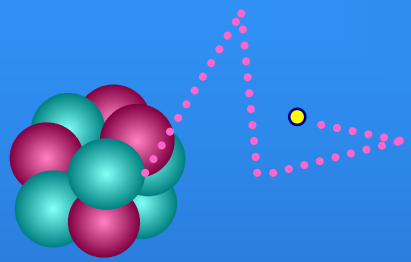

$P \longrightarrow N + e^{+} + n + \text{energy}$

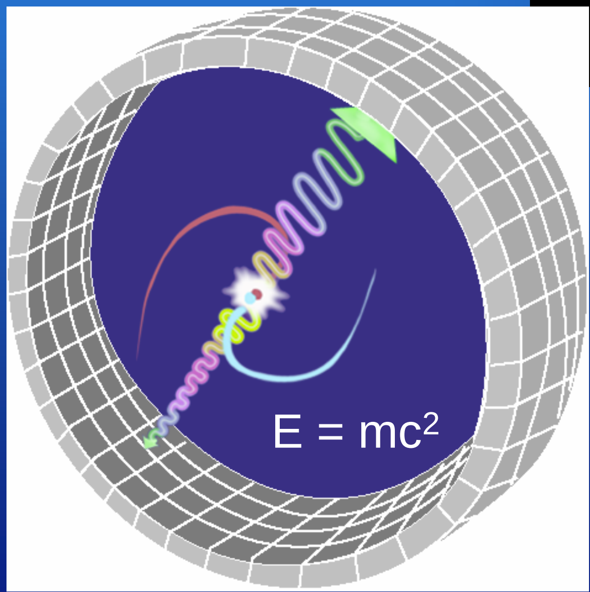

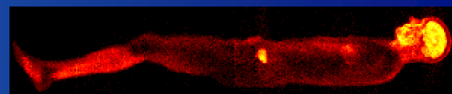

PET Isotopes

^{15}O

^{13}N

^{11}C

^{18}F

^{64}Cu

^{82}Rb

^{124}I

PET Tracers

$[^{15}O]$-O_2 $[^{15}O]$-H_2O

$[^{15}O]$-H_2O $[^{15}O]$-CO

$[^{13}N]$-NH_3 $[^{18}F]$-FDOPA

$[^{13}N]$-glutamate $[^{18}F^-]$

$[^{11}C]$-acetate $[^{18}F]$-FDG

$[^{11}C]$-palmitate

[11C]-methionine

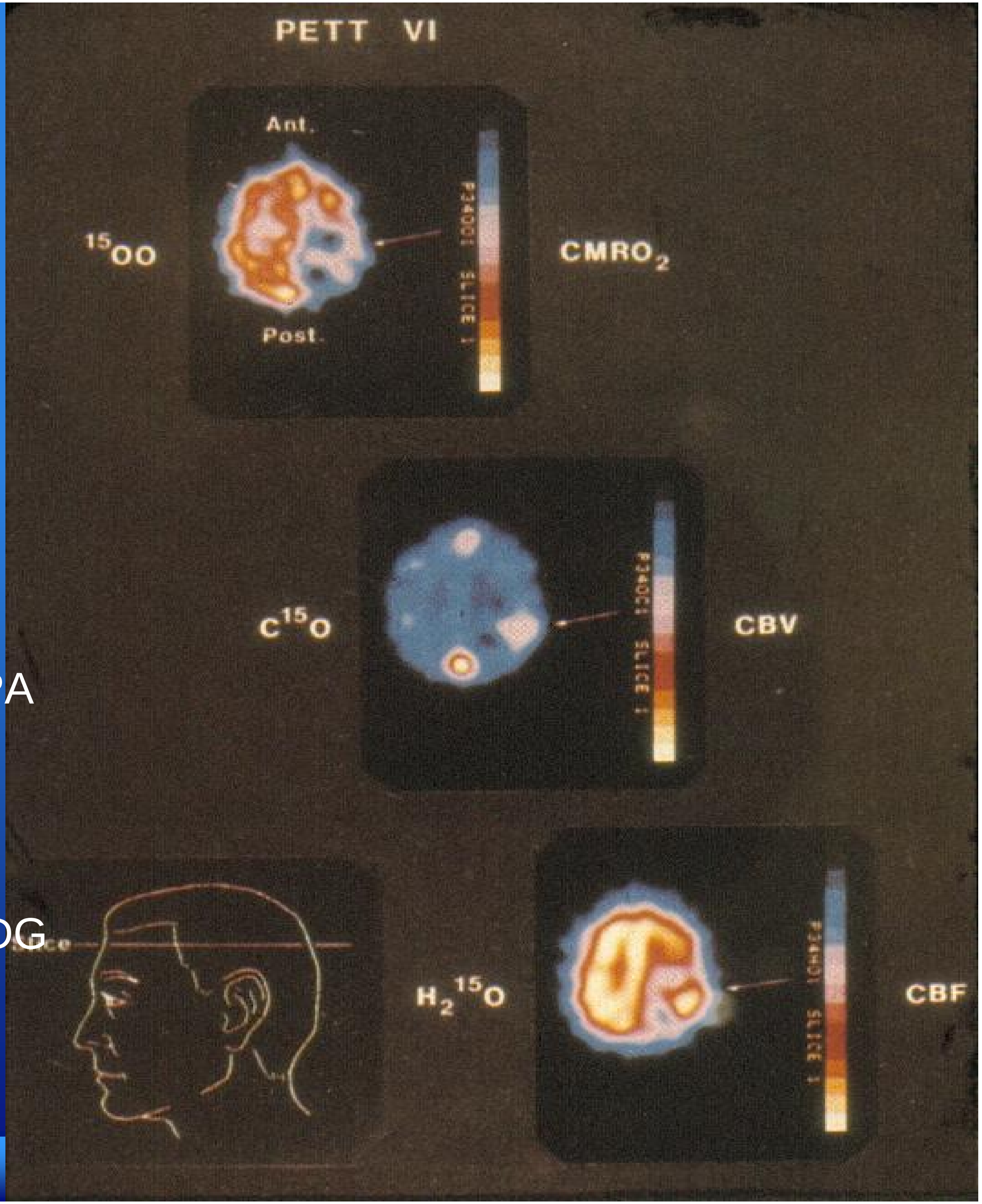

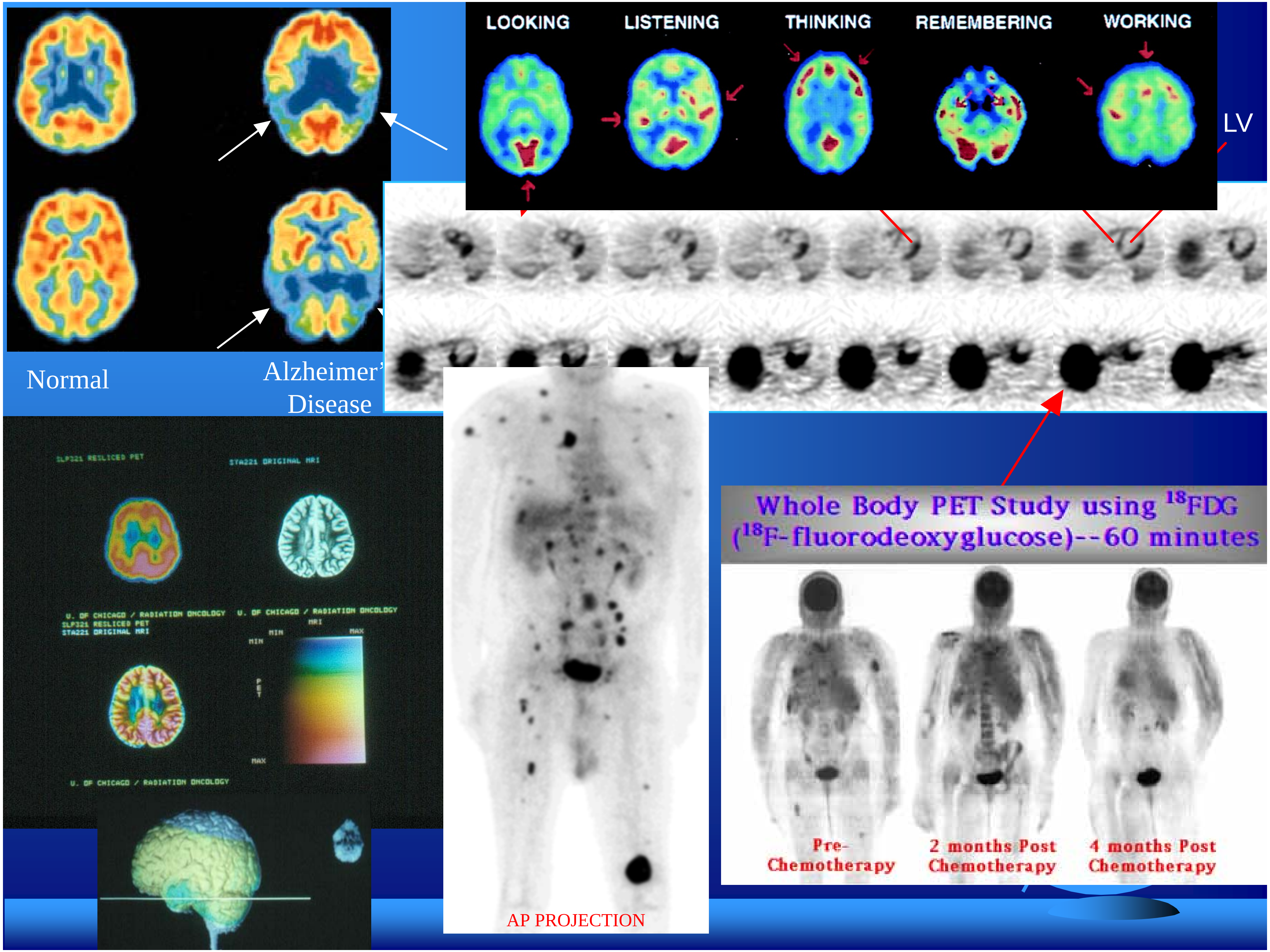

Normal
Alzheimer's Disease
LOOKING
LISTENING
THINKING
REMEMBERING
WORKING
LV
SLP321 RESLICED PET
STA221 ORIGINAL MRI
U. OF CHICAGO / RADIATION ONCOLOGY
SLP321 RESLICED PET
STA221 ORIGINAL MRI
U. OF CHICAGO / RADIATION ONCOLOGY
MRI
MIN
MAX
PET
U. OF CHICAGO / RADIATION ONCOLOGY
AP PROJECTION
Whole Body PET Study using 18FDG
(18F-fluorodeoxyglucose)--60 minutes
Pre-Chemotherapy
2 months Post Chemotherapy
4 months Post Chemotherapy

PET/CT Imaging

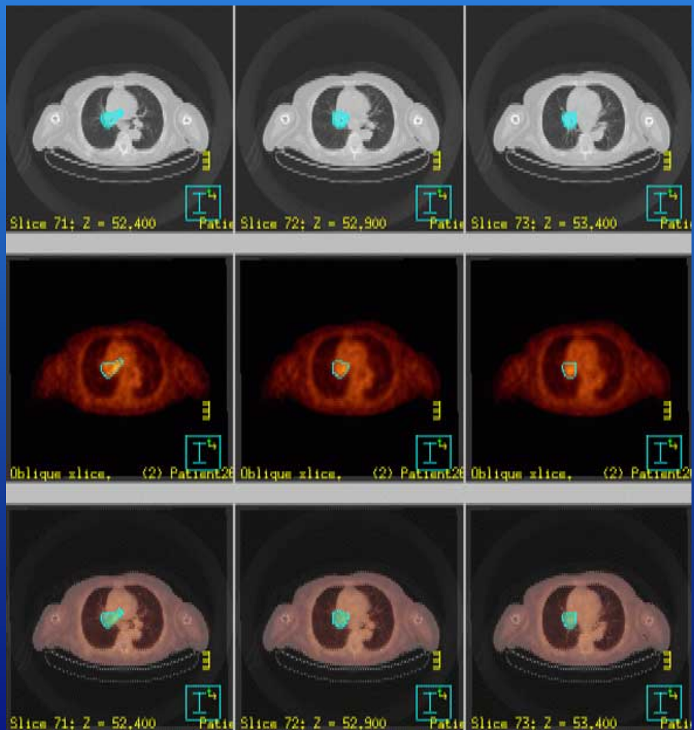

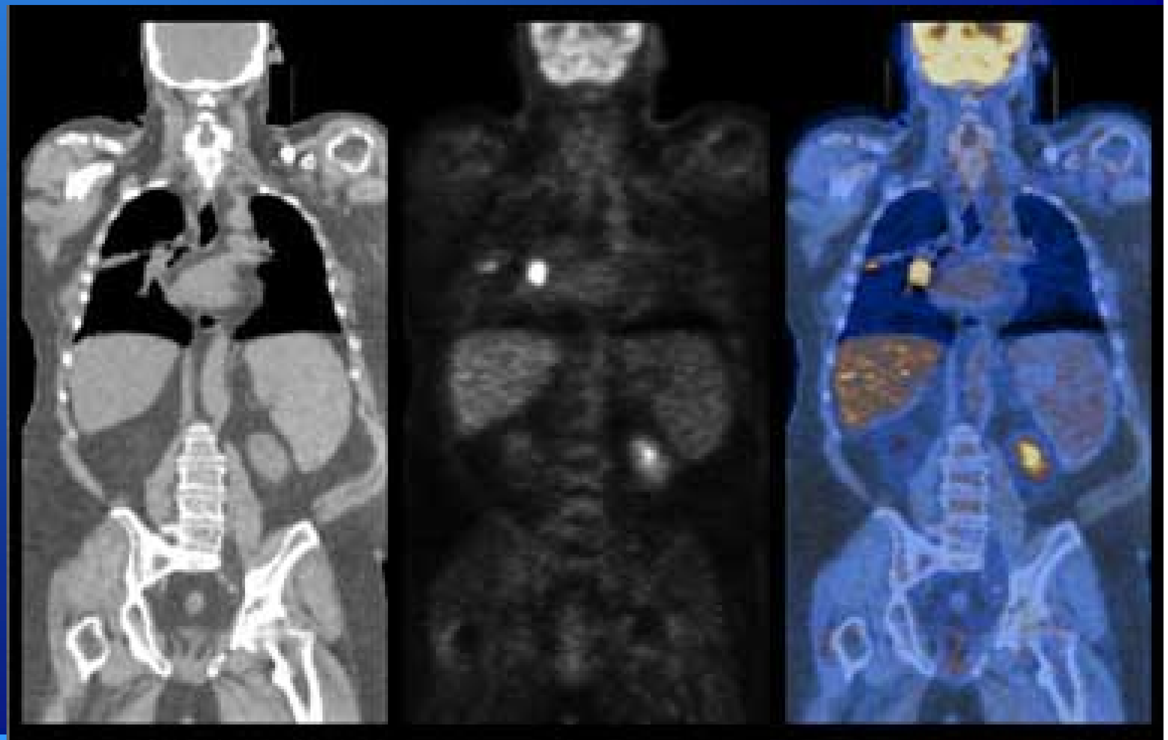

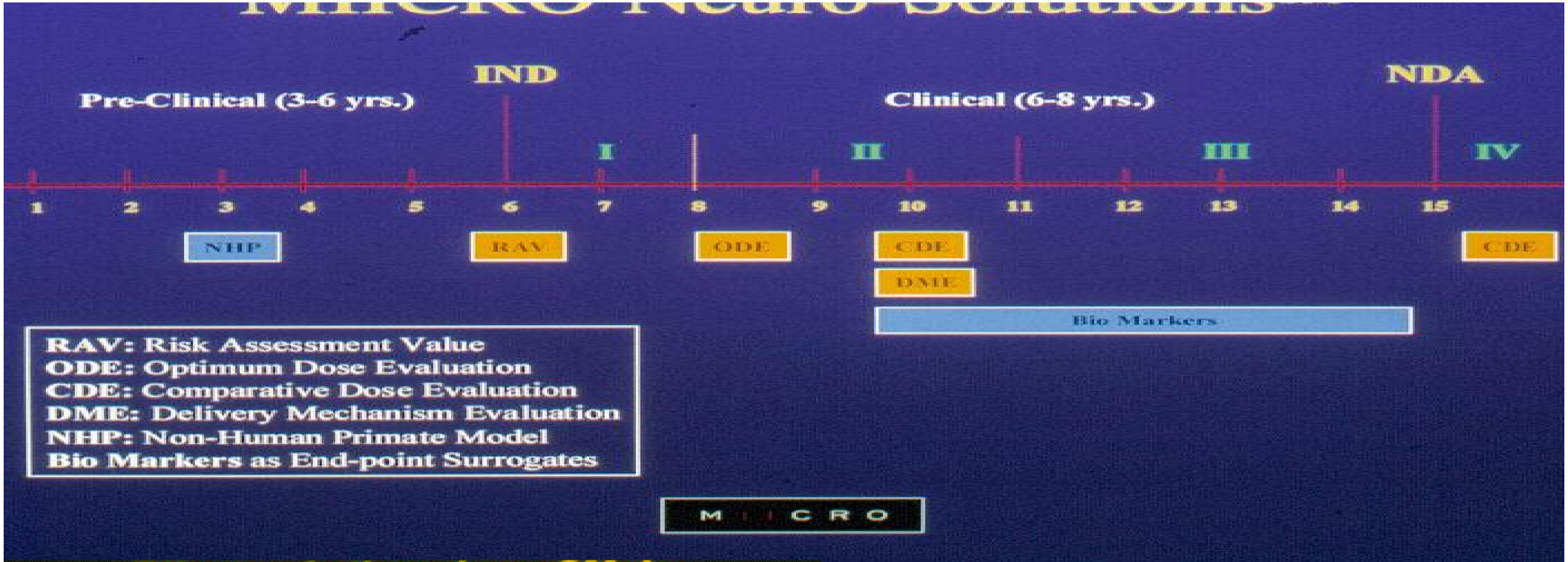
IND
NDA
Pre-Clinical (3-6 yrs.)
Clinical (6-8 yrs.)
I
II
III
IV
1 2 3 4 5 6 7 8 9 10 11 12 13 14 15
NHP
RAV
ODE
CDE
DME
Bio Markers
CDE
RAV: Risk Assessment Value
ODE: Optimum Dose Evaluation
CDE: Comparative Dose Evaluation
DME: Delivery Mechanism Evaluation
NHP: Non-Human Primate Model
Bio Markers as End-point Surrogates
MICRO

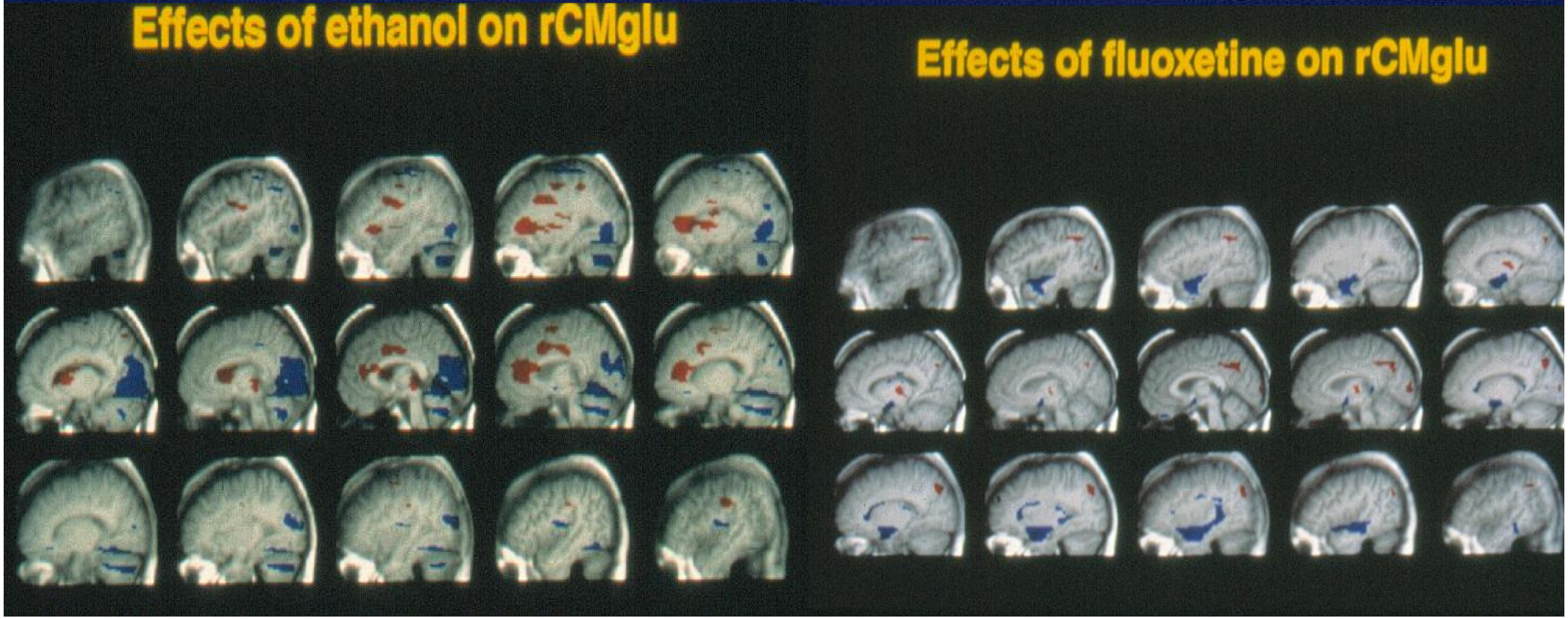
Effects of ethanol on rCMglu
Effects of fluoxetine on rCMglu

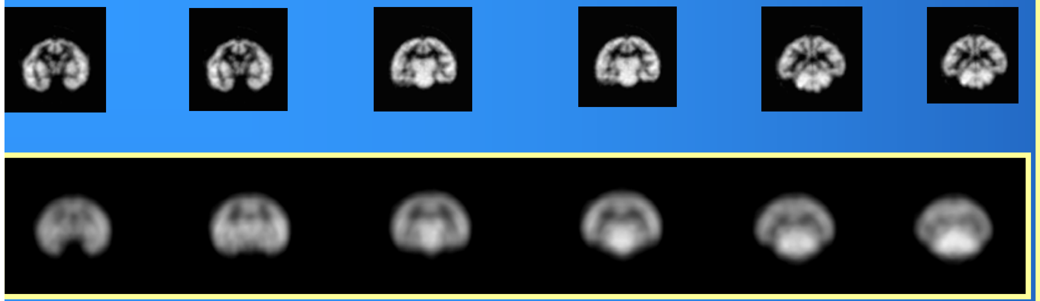

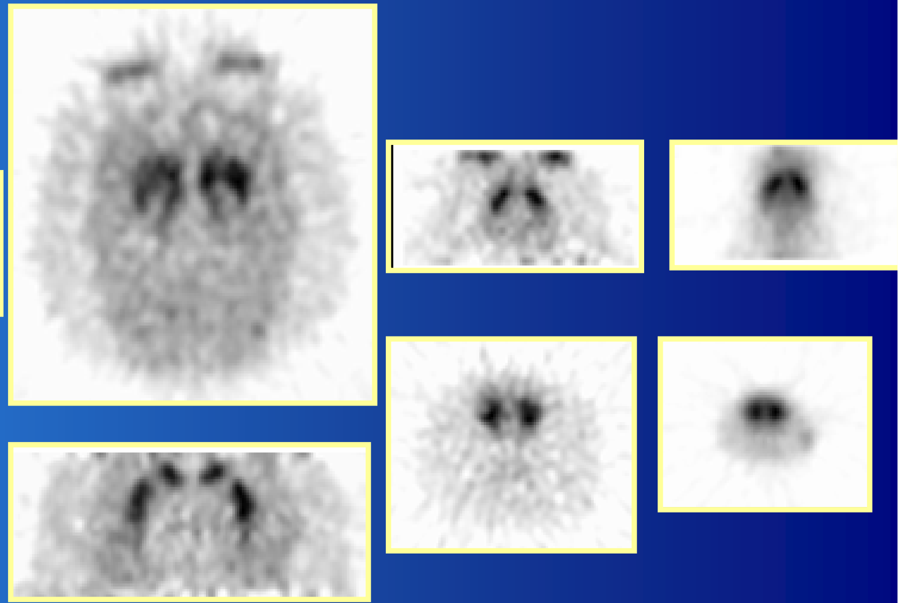

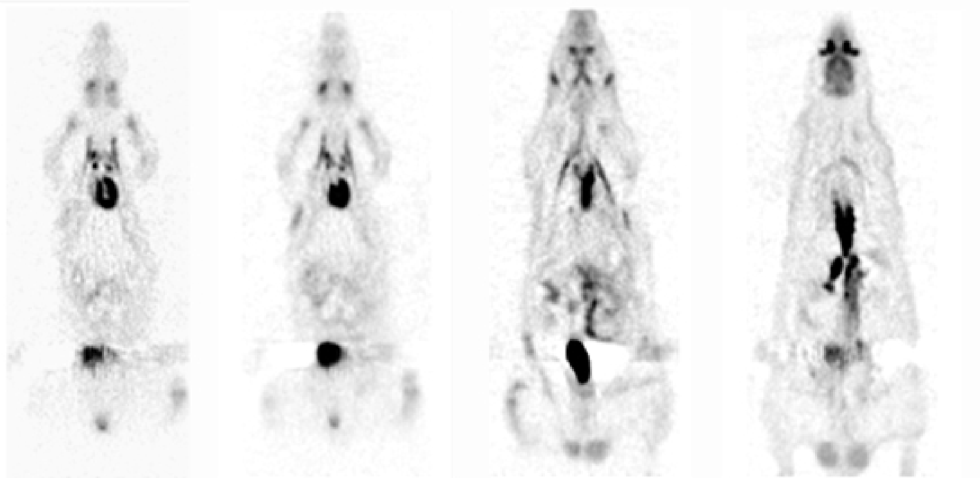

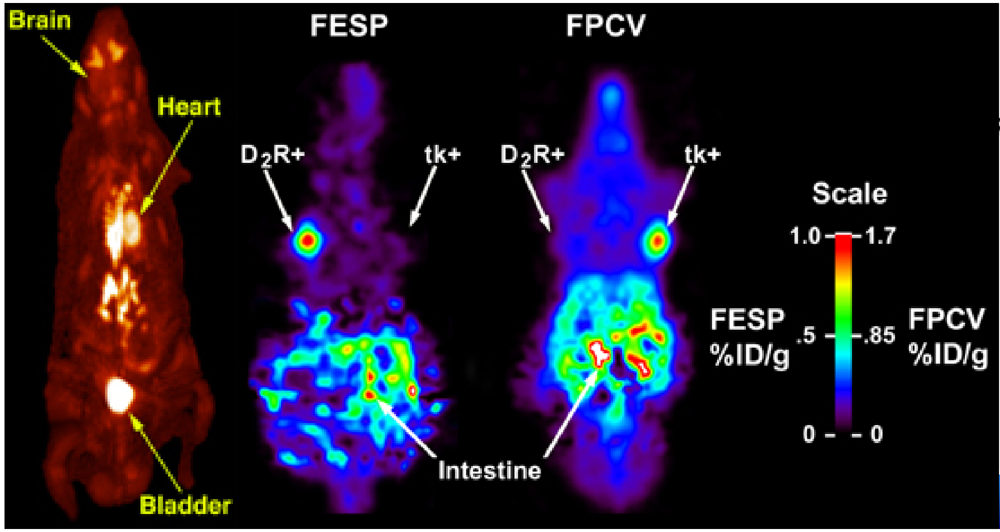
Brain
Heart
Bladder
FESP
FPCV
D_2R+
tk+
D_2R+
tk+
Intestine
Scale
1.0
1.7
.5
.85
0
0
FESP
%ID/g
FPCV
%ID/g

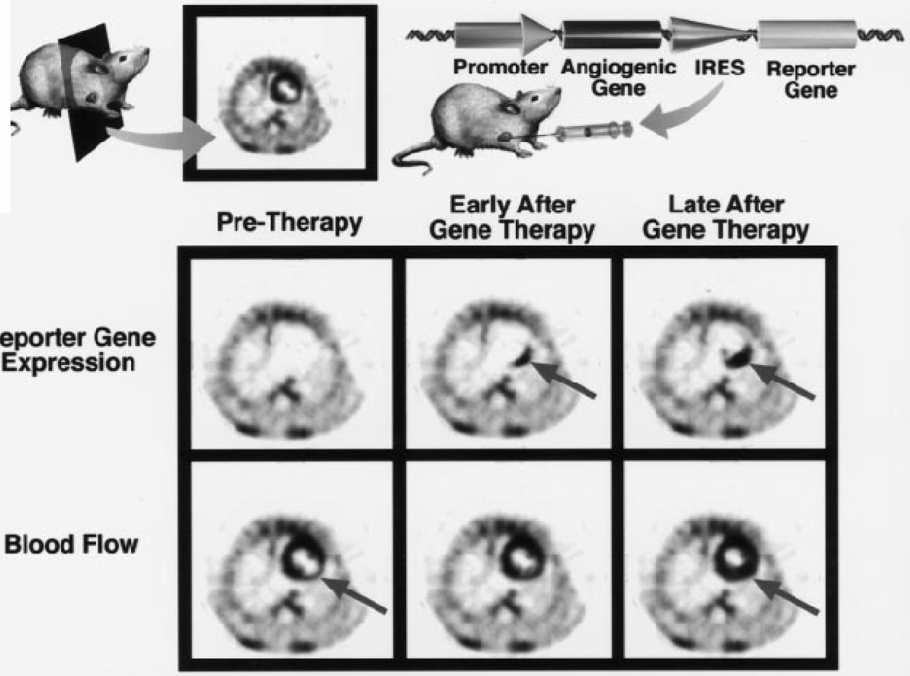
Promoter
Angiogenic Gene
IRES
Reporter Gene
Pre-Therapy
Early After Gene Therapy
Late After Gene Therapy
Reporter Gene Expression
Blood Flow

Biochemical Imaging with Small Animals

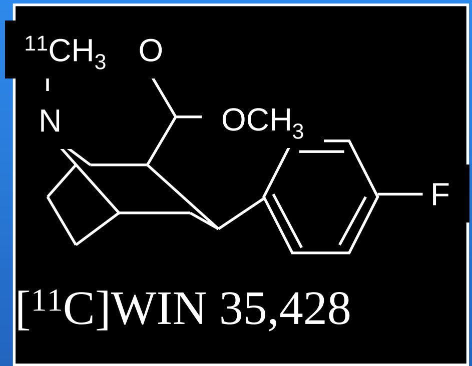

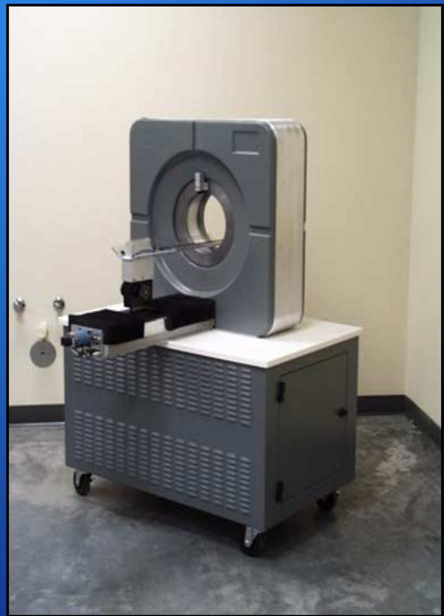

microPET

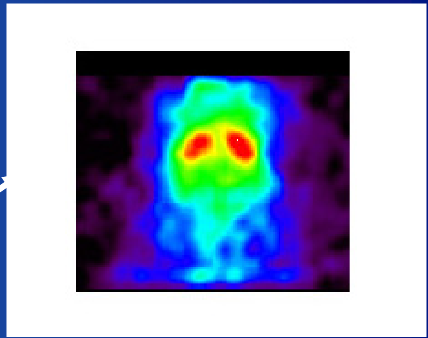

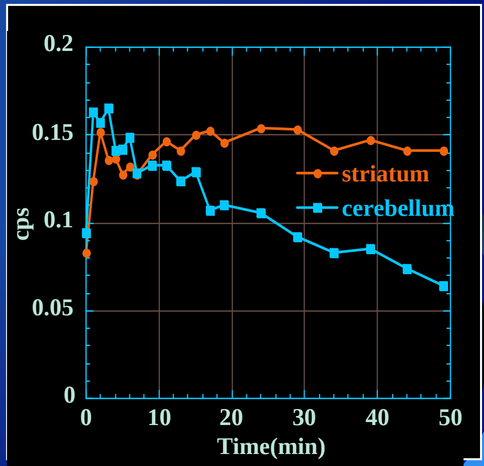

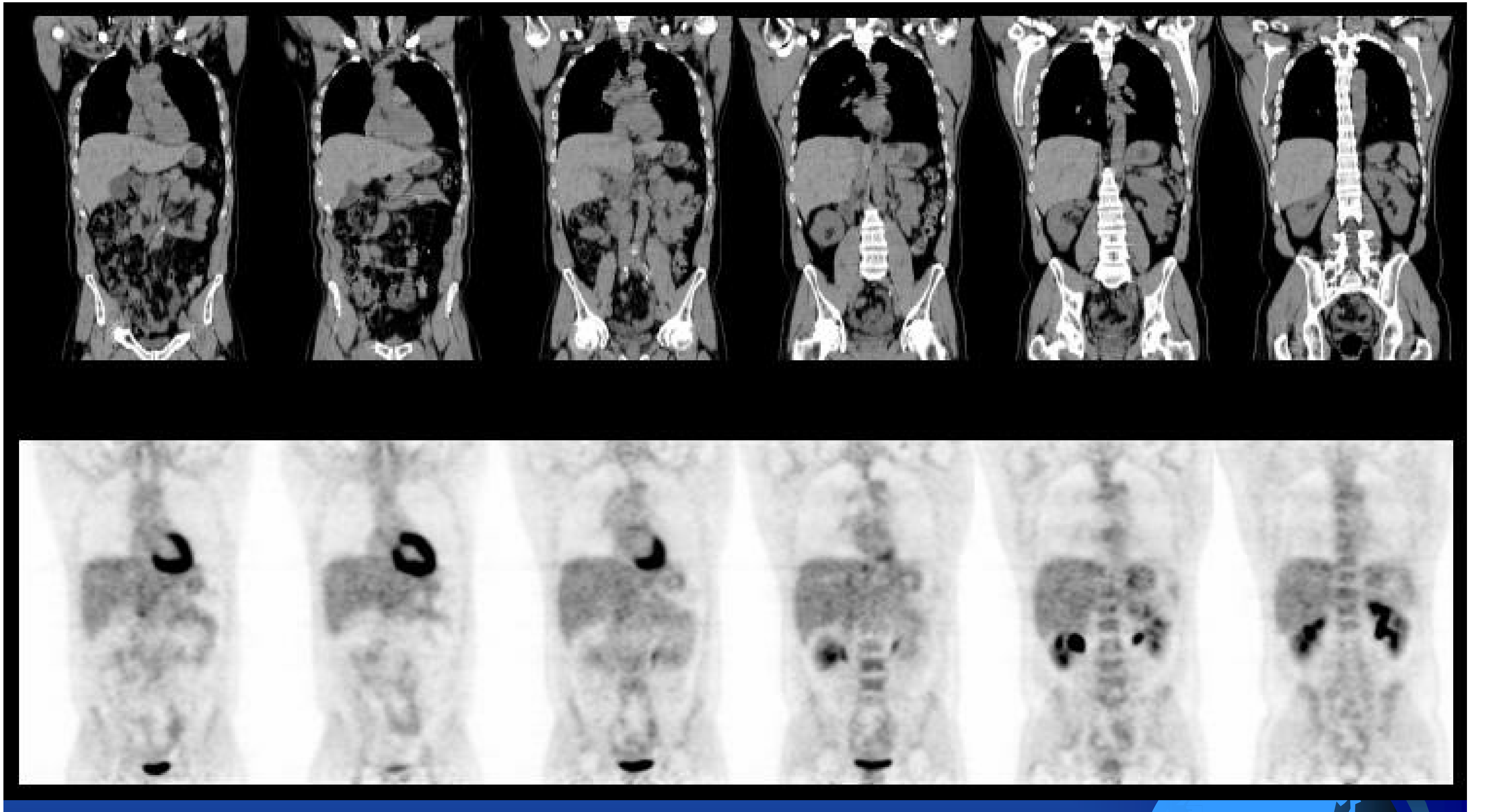

Human PET: 3-4mm; Target: 1-2mm
Animal PET: 1-2 mm; Target: <0.5mm

Multi-Modality Integrative System

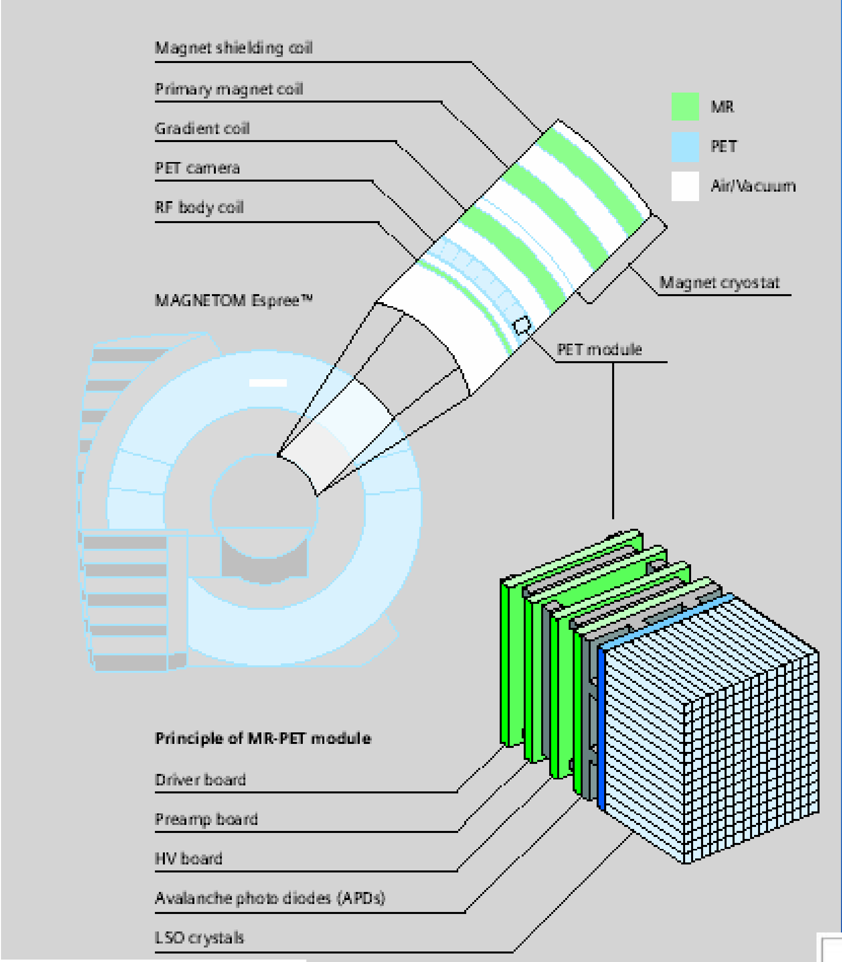

PET/MRI

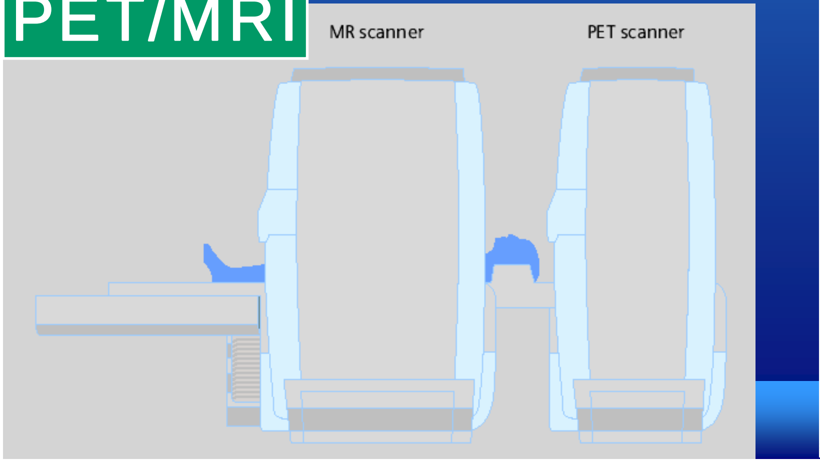

PET/SPECT

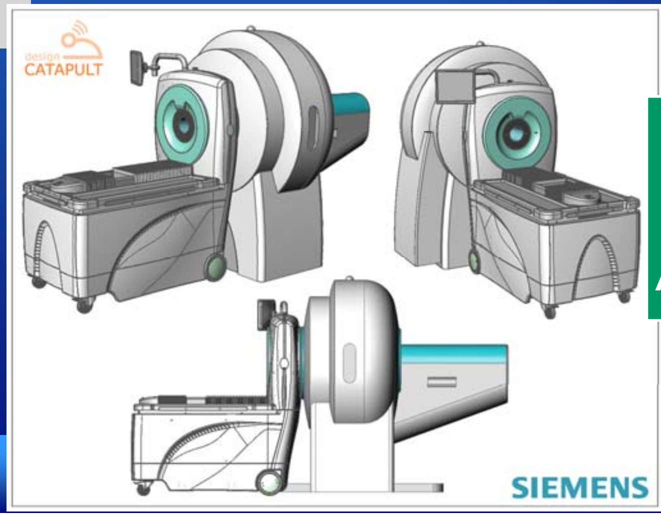

PET/SPECT/CT
For
Animal Imaging

Siemens "Molecular Imaging"

Investigation of Scatter in PET Using SimSET

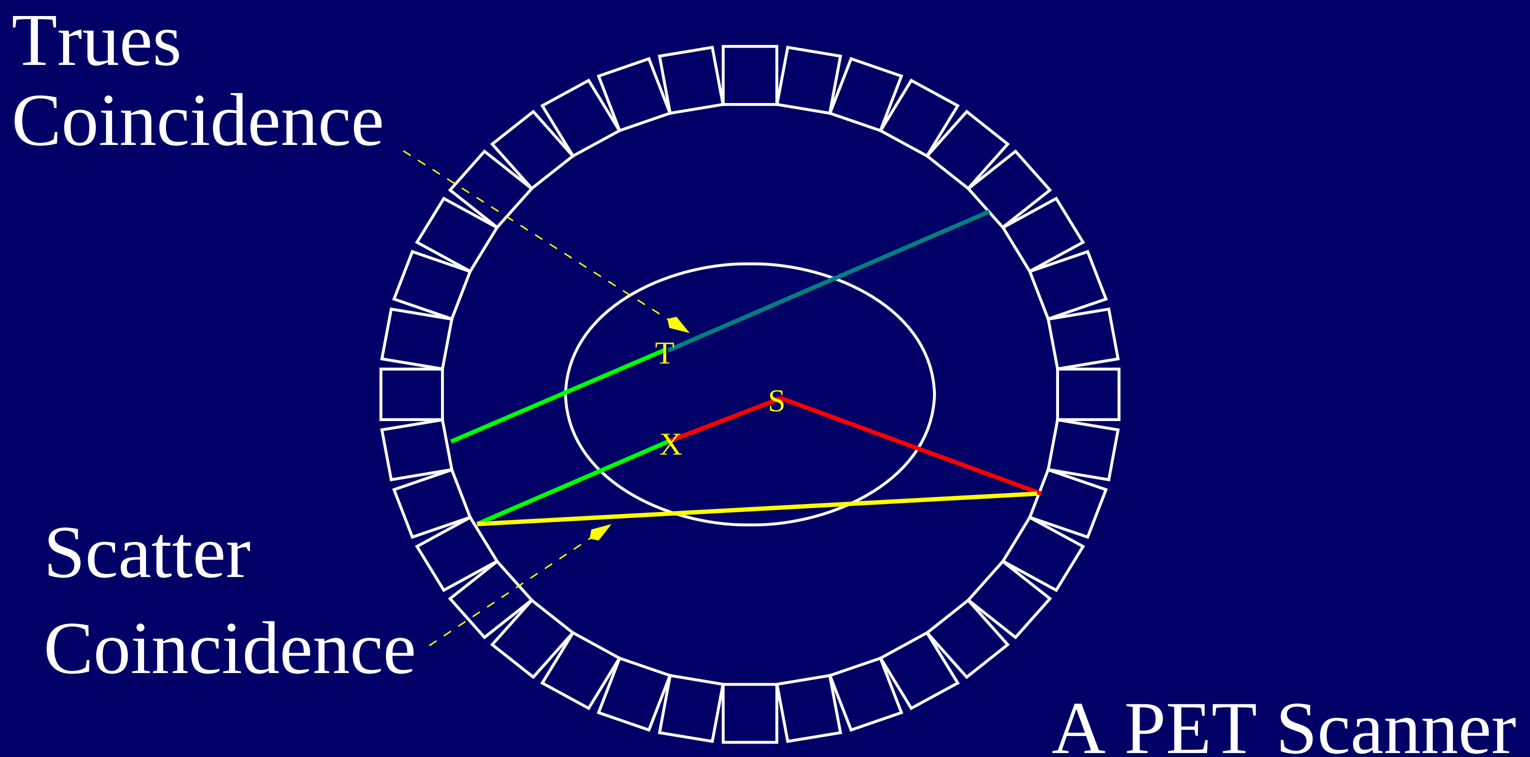

Effect of scatter on image

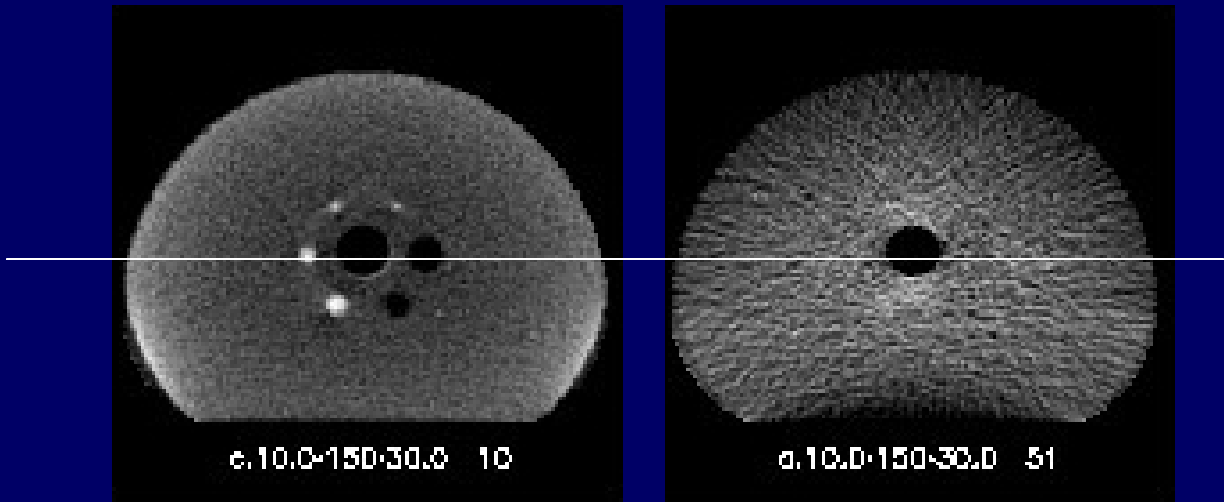

Trues **Raw**

Raw = Trues + Scatter

Effect of scatter on image

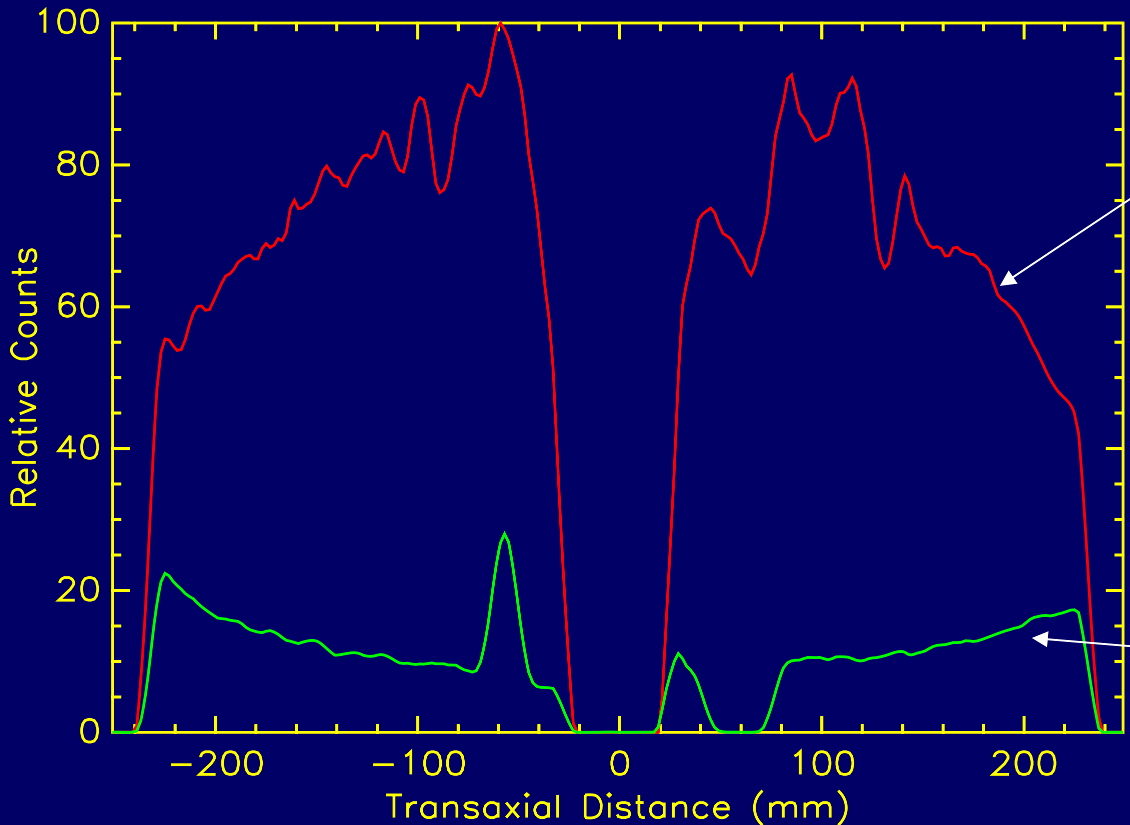

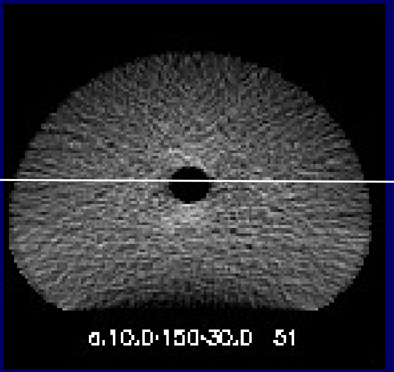

Raw

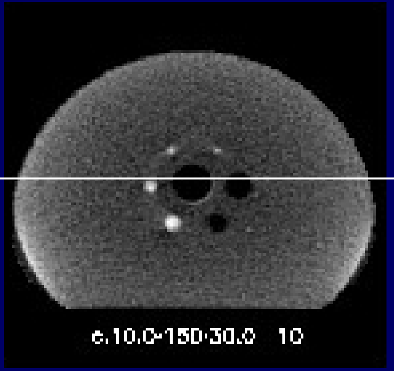

Trues

TFF *vs.* object shape

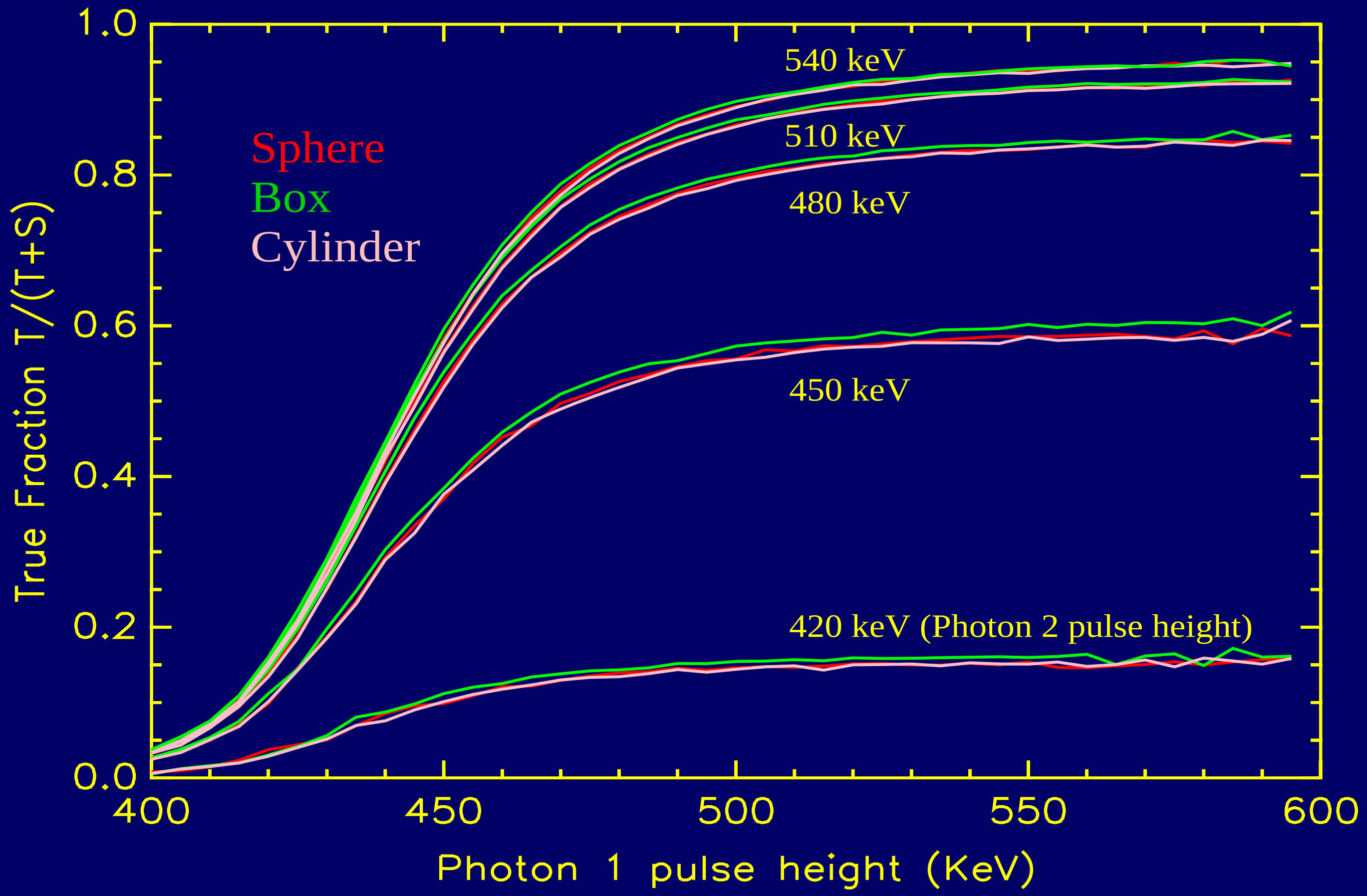

scanner: 7.5 cm inner radius, 15% resolution

\

TFF *vs.* object size

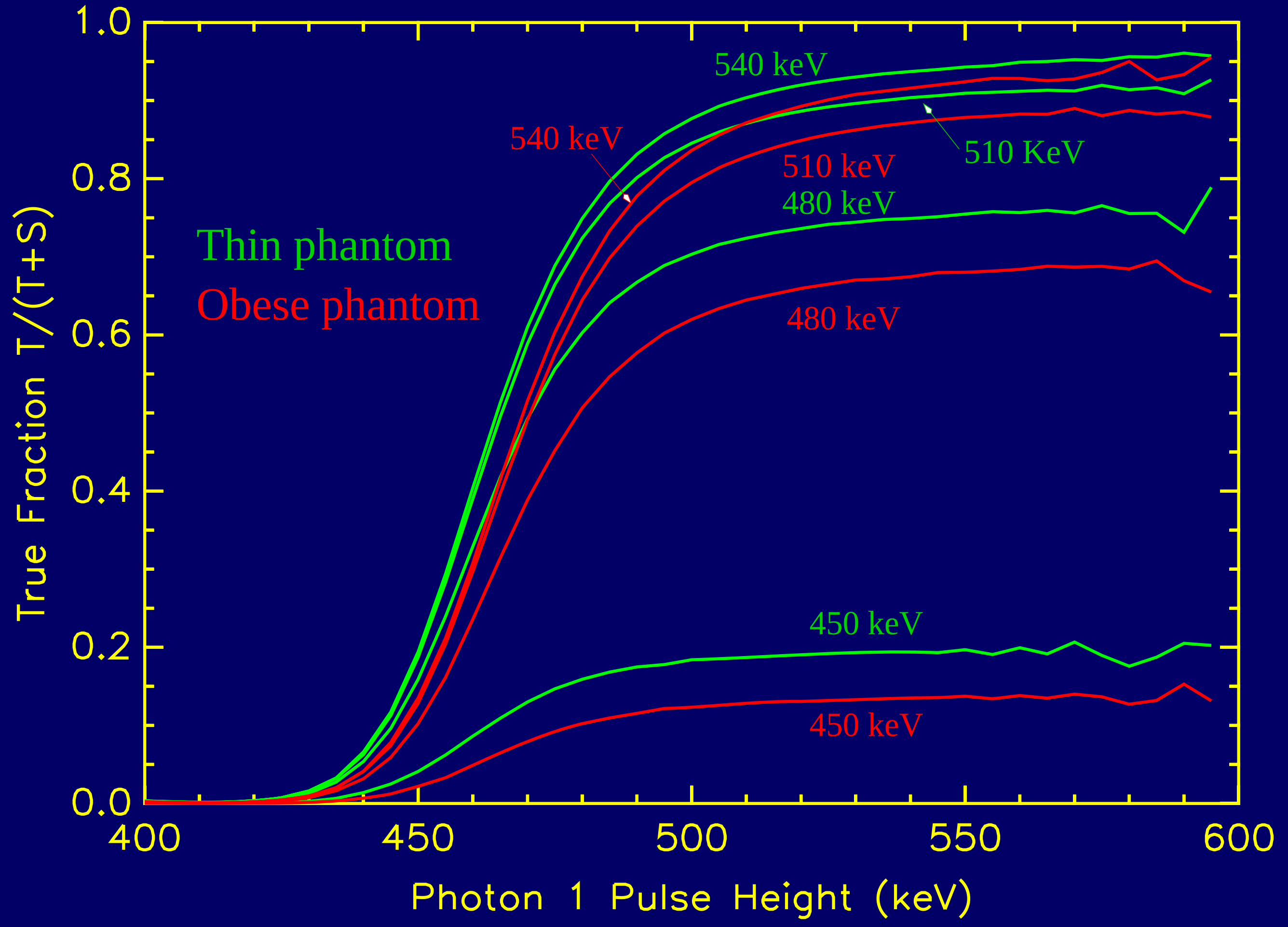

10% energy resolution, large scanner

\

TFF *vs.* scanner radius

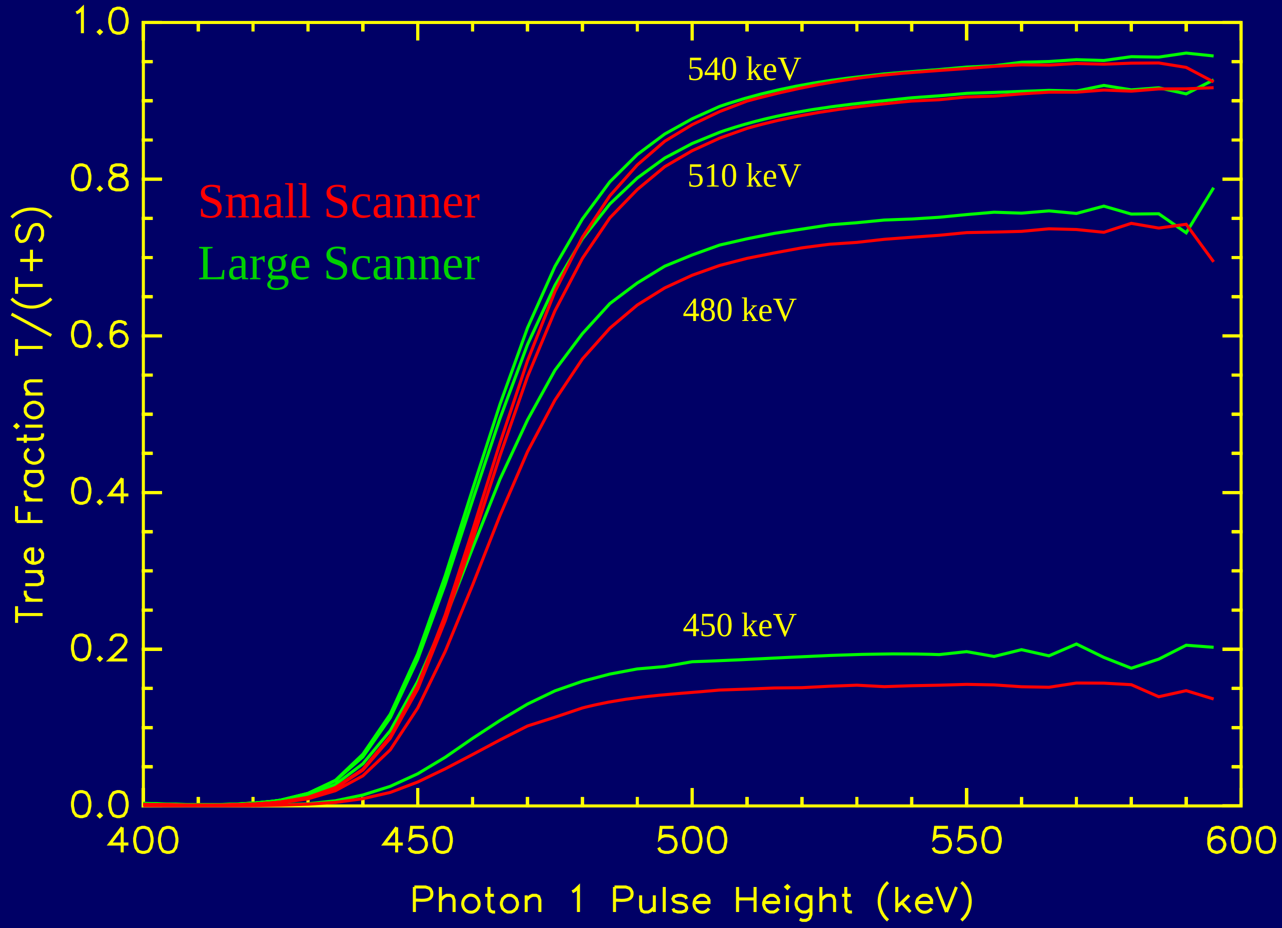

thin phantom
10% energy
resolution

\

Thin phantom in the large scanner

LLD =
150 keV

LLD =
350 keV

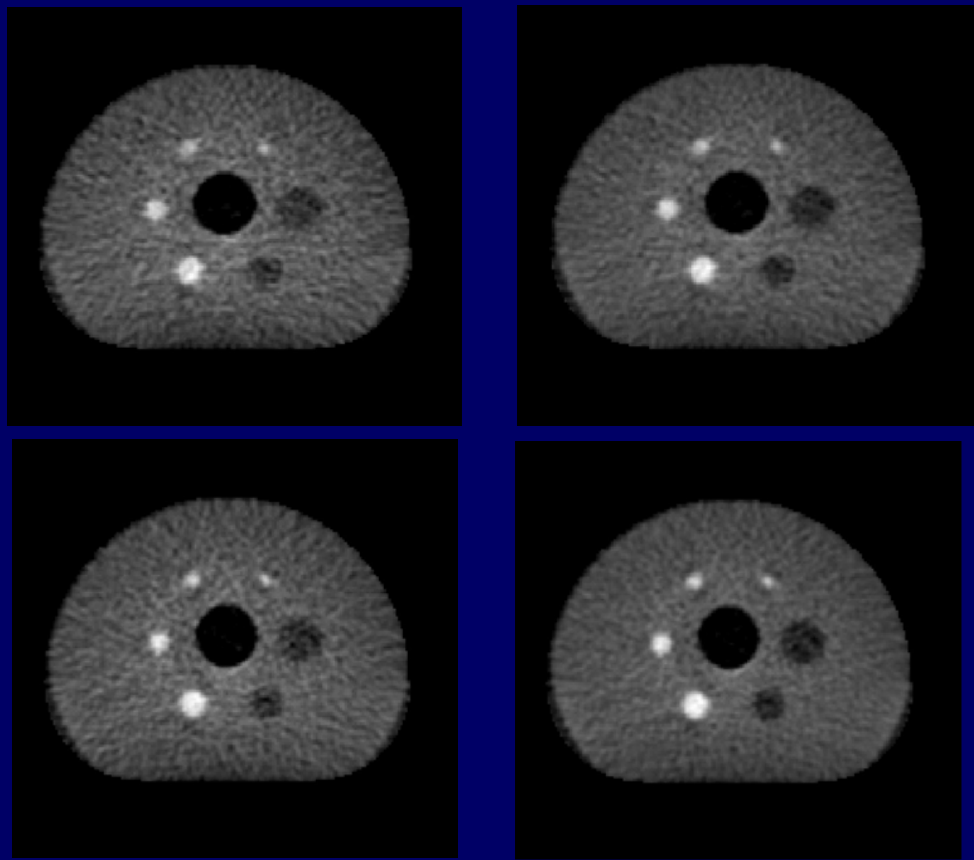

raw corrected

Obese phantom in the small scanner

LLD =
150 keV

LLD =
350 keV

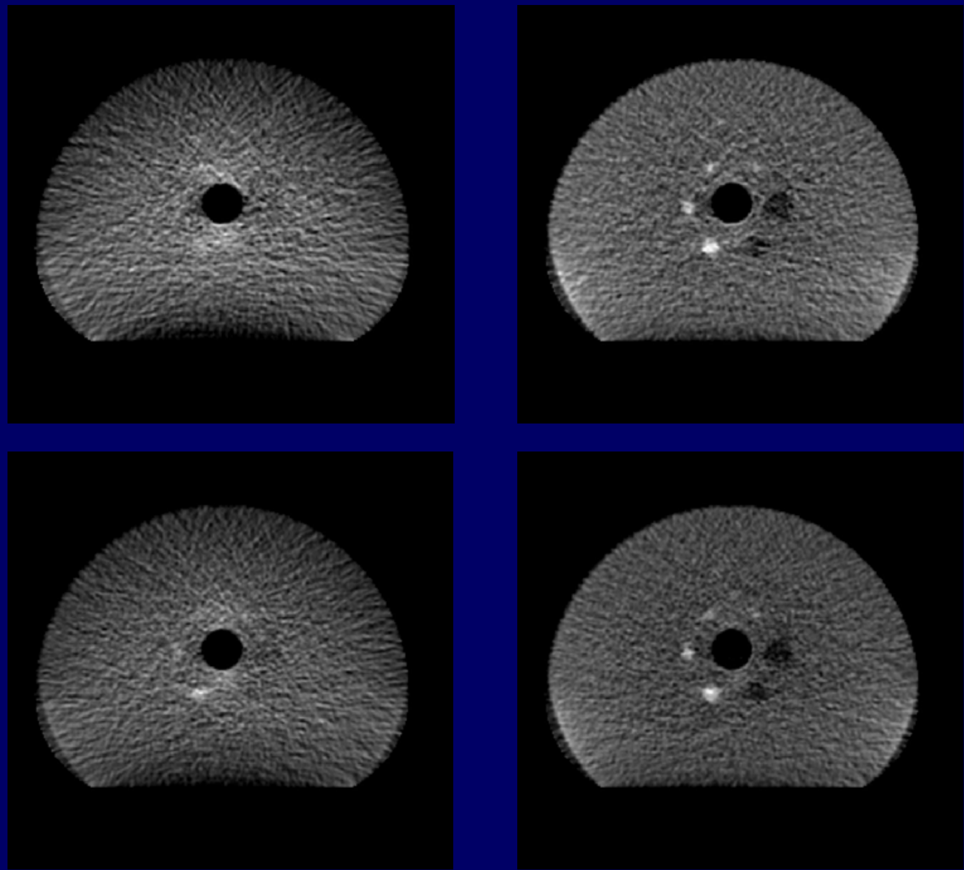

raw

corrected

\

Dual-Head microPET Prototype SimSET

\

Sensitivity

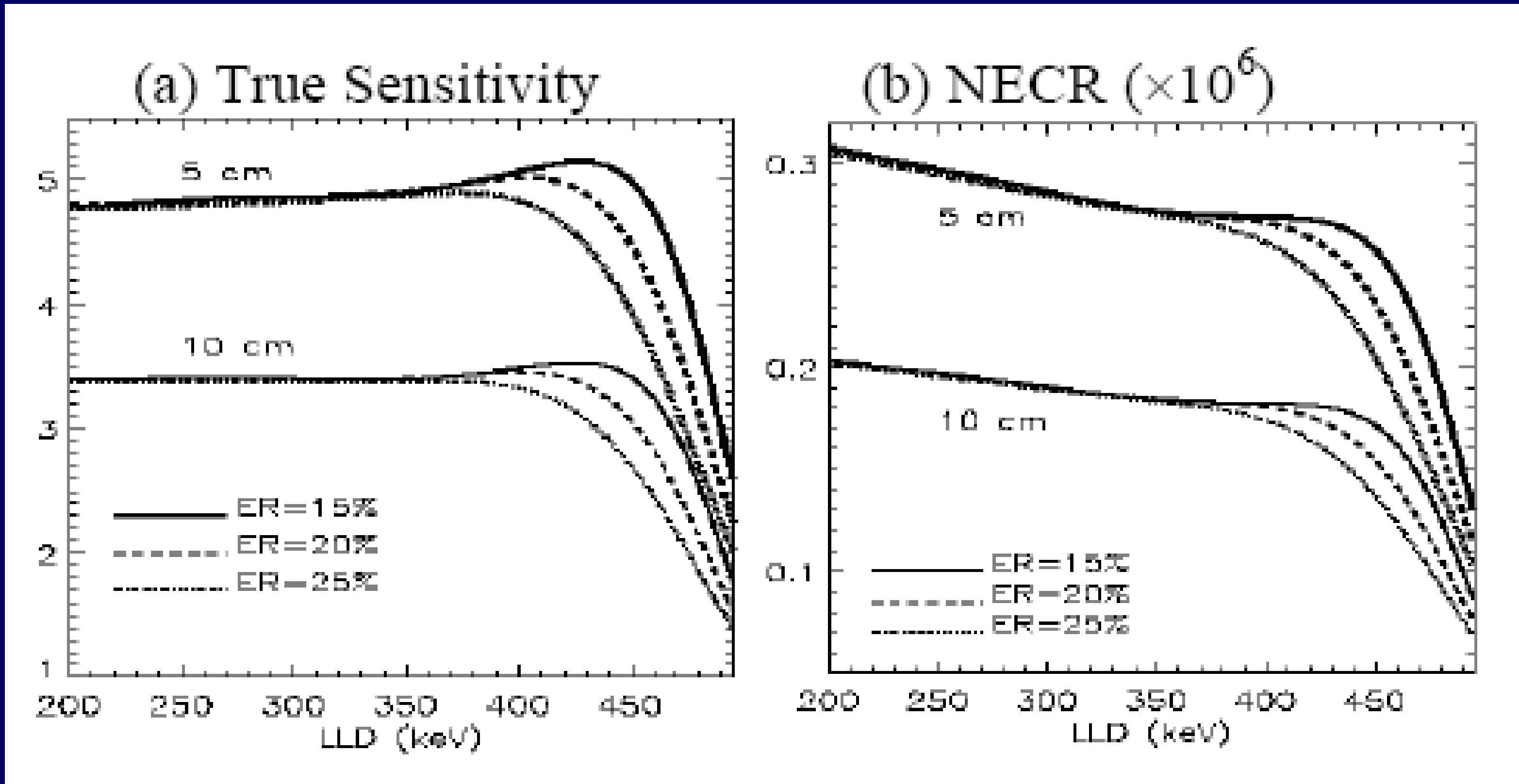

\

Flexible Configuration

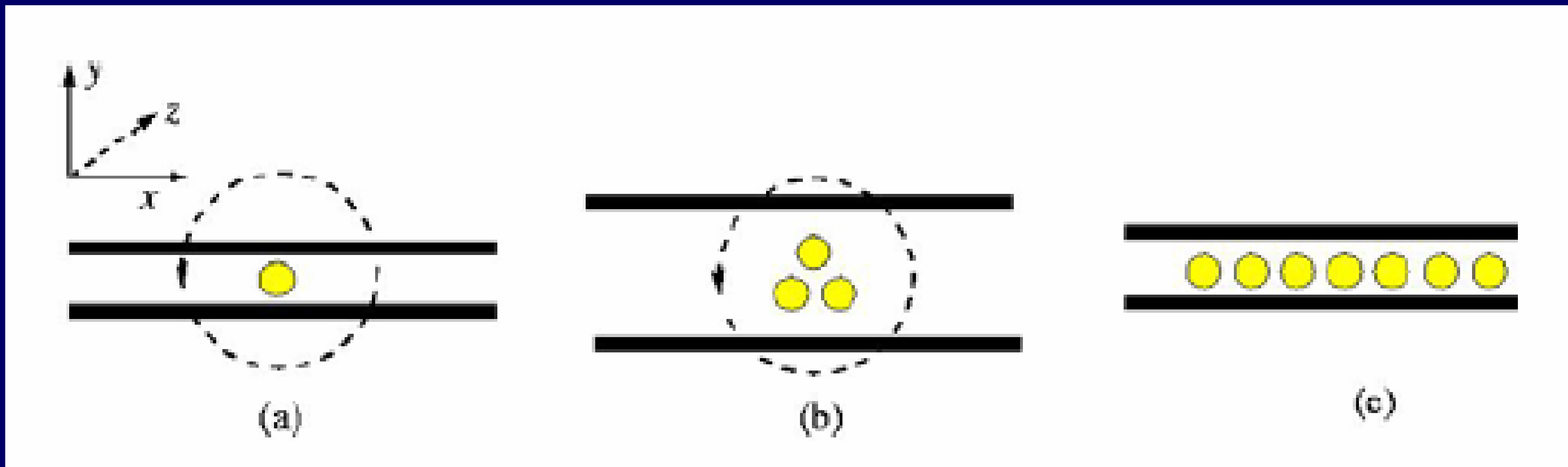

\

Example Reconstruction

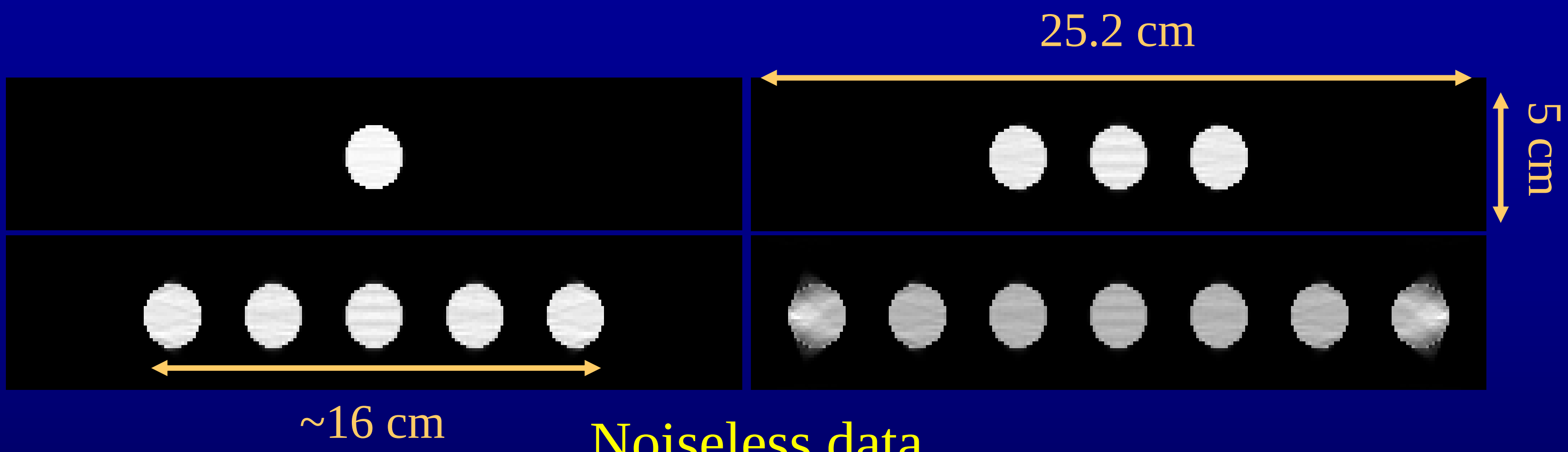

Noiseless data

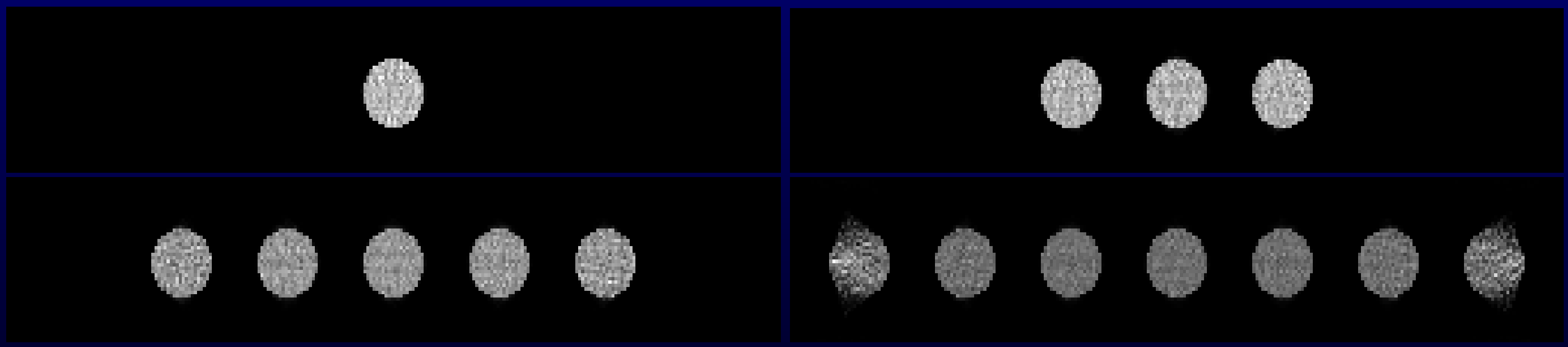

Noisy data

Time-of-Flight Tomograph

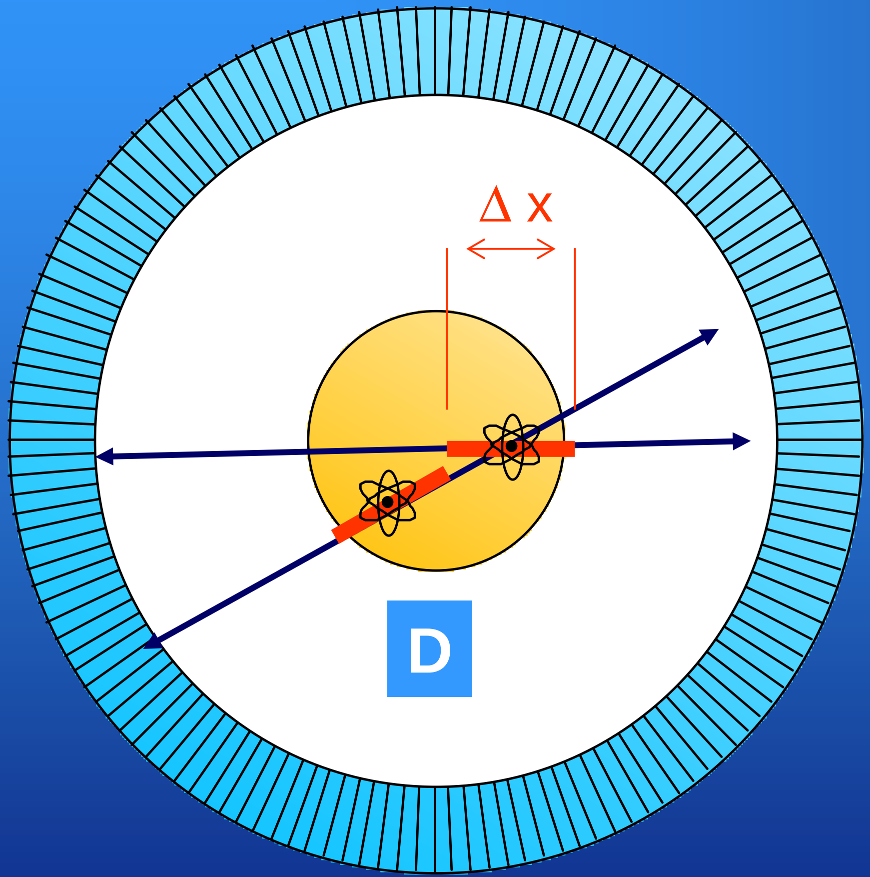

- Can localize source along line of flight - *depends on timing resolution of detectors*
- Time of flight information can improve signal-to-noise in images - *weighted back-projection along line-of-response (LOR)*

Δ x = uncertainty in position along LOR
= c · Δt/2

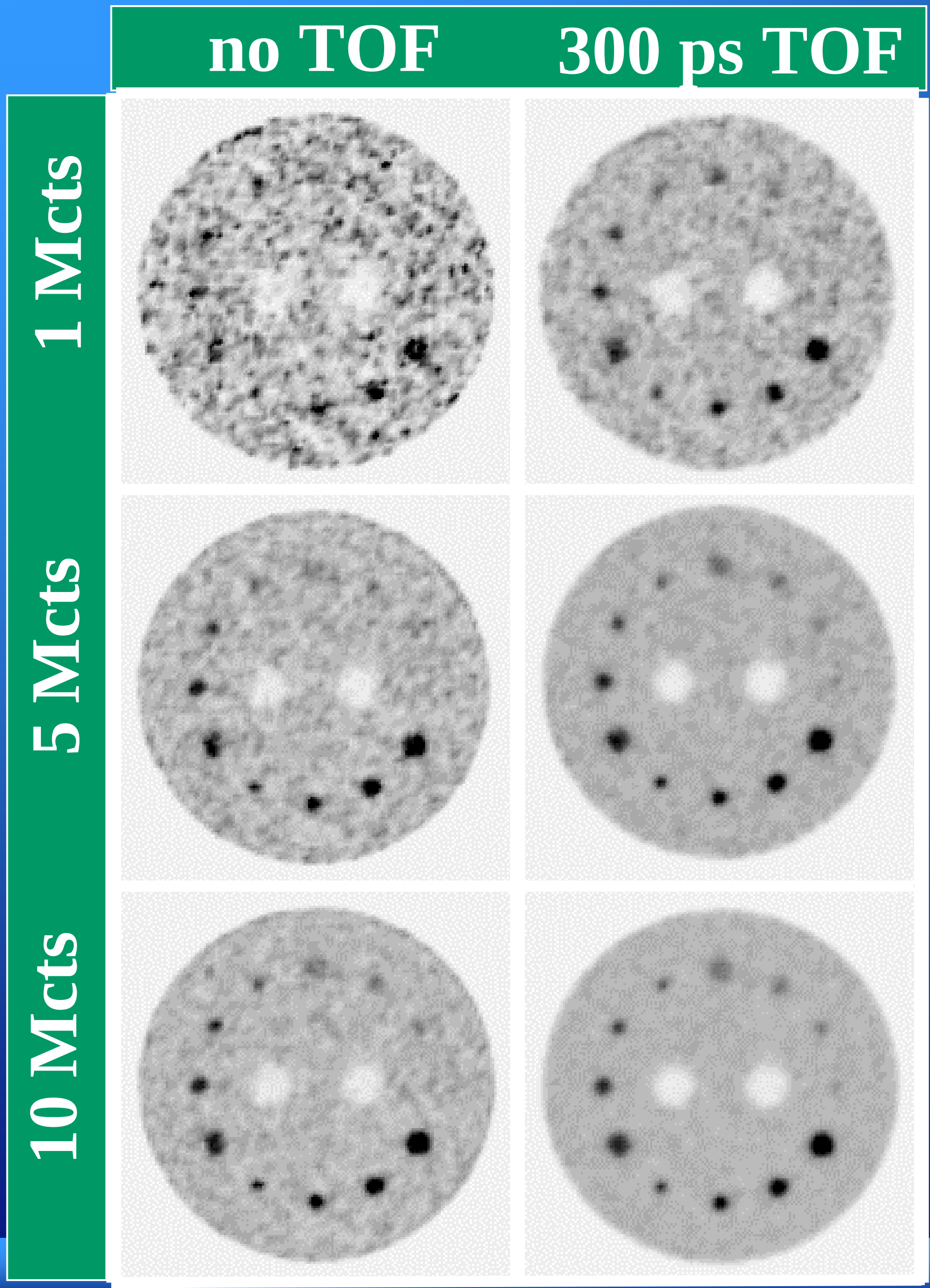

Benefit of TOF

Better image quality
Faster scan time

5Mcts TOF	5Mcts
1Mcts TOF	1Mcts

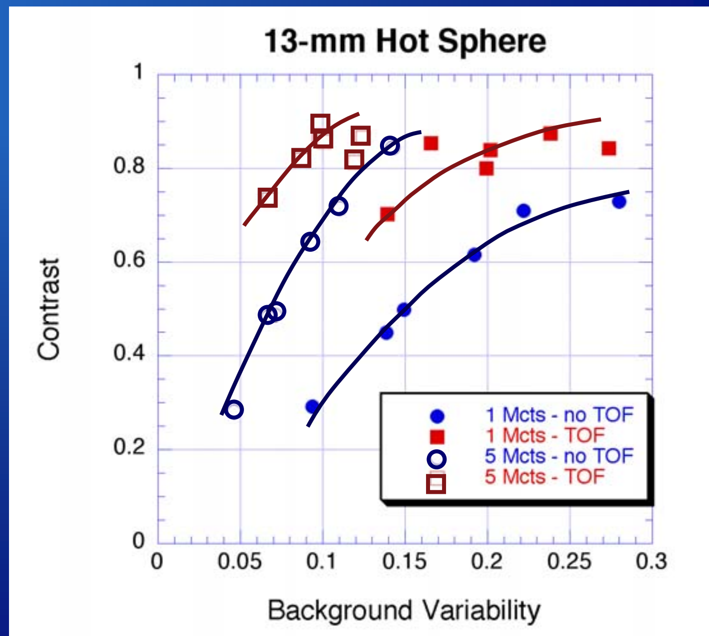

Karp, et al, UPenn

Questions

- Smaller CW reduces randoms, scatter, and trues, at different rates. *Is it beneficial to employ CWs much smaller than those currently being used, even though it is much smaller than the object size?*

- In detector design, one could make a compromise between timing resolution and other performance characteristics such as energy resolution. Therefore: *In TOF-PET imaging, is it possible to trade energy resolution for timing resolution in such ways not diminishing, or even leading to improved, image quality?*

Methods

◆ GATE Simulation

❖ PET:

- 82.5 cm ring diameter, 16.2 cm axial length
- 24 transaxial rings made of $6.45\times6.45\times25mm^3$ LSO crystals
- 1mm thickness and 66.5mm length septa
- ~60 cm diameter FOV

❖ Phantom:

- 40cm diameter, 16.2cm height cylinder
- containing uniform activity of ~6.3KBq/cc

❖ Data generation: Perfect timing and energy resolution single events were generated by GATE. We then re-sampled the arrival times and detected energies of the simulated single events with Gaussian distributions to obtain specific energy resolutions (ER) and timing resolutions (TR). Various coincidence windows (CWs) are applied to obtained coincidence events.

Results

CW	600 ps		1 ns		1.4 ns		2 ns	
system	better-T_r	better-E_r	better-T_r	better-E_r	better-T_r	better-E_r	better-T_r	better-E_r
SF	25.4%	19.7%	26.7%	20.2%	27.4%	20.6%	27.6%	20.8%
RF	8.6%	6.8%	10.4%	7.8%	12.9%	9.4%	17.3%	12.4%
NEC($\times 10^8$)	8.308	7.372	1.056	1.001	1.100	1.099	1.053	1.095

Table 1: Detection performance of two systems when employing various CWs (better-T_r system: $E_r = 30\%$, $T_r = 300$ ps; better-E_r system: $E_r = 10\%$, $T_r = 700$ ps).

- ❖ SF is larger with the 300ps TR, 30% ER case.
- ❖ RF increases with the coincidence window
- ❖ NEC reaches maximum at CW~1.4ns

Table 2. TR300ps-ER30% vs. TR700ps-ER15% with CW600ps,1000ps,1400ps,2ns,4ns

	T		S		R		SF		RF		NEC(T*T/(T+S+R))	
	TR 300ps	TR 700ps	TR 300ps	TR 700ps	TR 300ps	TR 700ps	TR 300ps	TR 700ps	TR 300ps	TR 700ps	TR 300ps	TR 700ps
CW 600ps	1193024	971741	407812	238162	112423	70961	0.254749	0.196844	0.086118	0.068055	830759.5	737221.6
CW 1000ps	1563243	1339122	569126	338889	181539	114119	0.266898	0.201959	0.104047	0.078527	1056105	1000624
CW 1400ps	1678664	1498403	633214	388928	248906	155543	0.273896	0.206073	0.129129	0.094044	1100410	1099046
CW 2000ps	1673307	1538692	636742	404497	349924	218476	0.27564	0.208161	0.172953	0.124334	1052626	1095254
CW 4000ps	1617618	1486504	615967	390694	672932	419189	0.275775	0.208126	0.293786	0.219967	900283.1	962248.1

Results

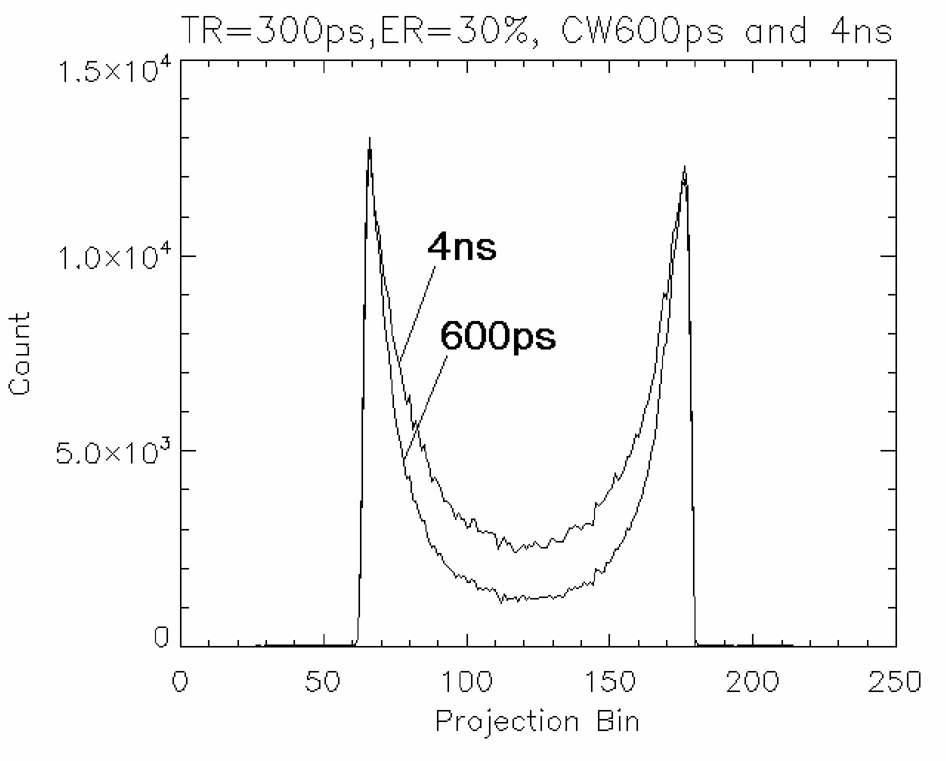

Figure 1(a) T events

Fig.1(a,b,c) Profiles of the trues (T), scatter (S), and randoms (R) profiles obtained for TR=300ps, ER=30%, using CW=600ps or 4ns. All time bins are summed and these profiles correspond to the non-TOF case. The coincidence window is observed to affect spatial distributions of trues and scatter. The spatial distribution of the randoms remain spatially uniform with both coincidence windows.

Results

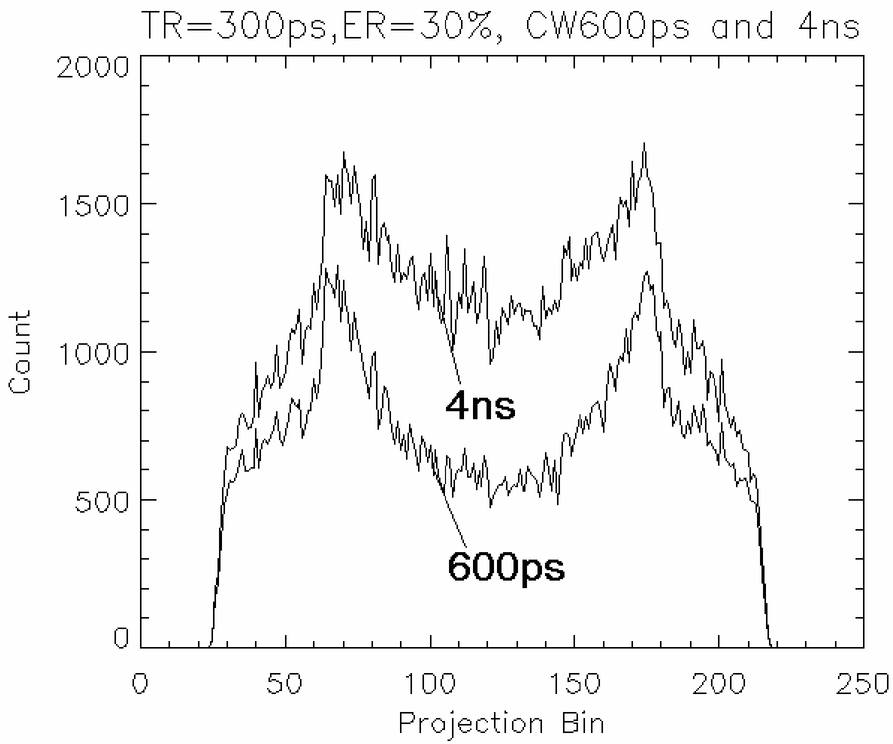

Figure (b) S events

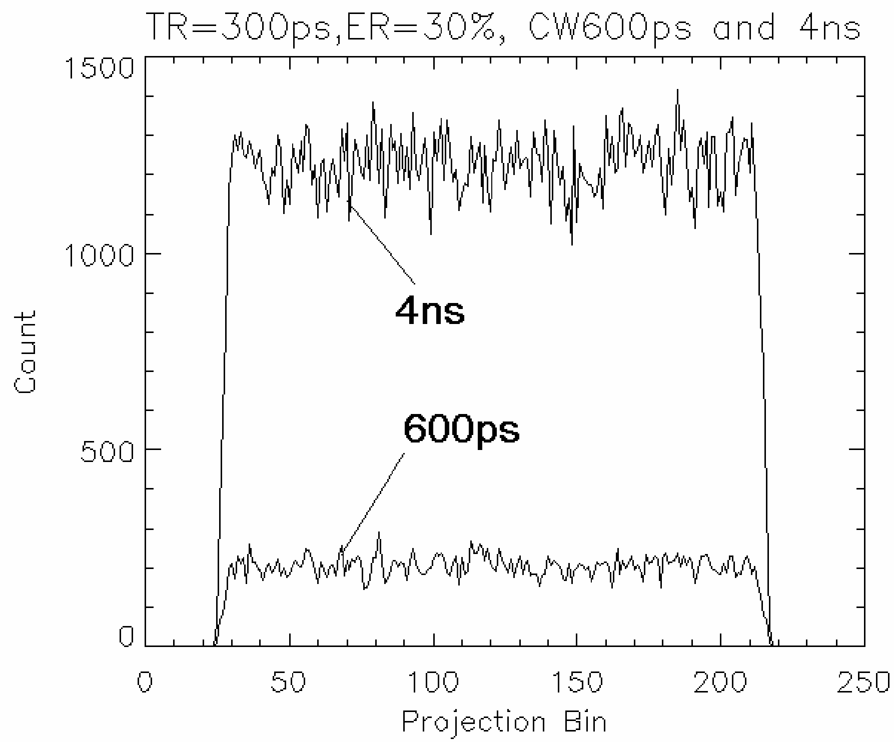

Figure 1(c) R events

Reconstructed Image

- **Reconstruction:** the EM algorithm, 50 iterations, with attenuation correction and smoothing introduced during iteration

- Cases considered:
  - NON-TOF PET: CW=4ns
  - TOF-PET: CW=600ps, 1ns, 1.4ns, 2ns

- Images are obtained by using
  - trues only (T images)
  - trues+scatter (T+S images)
  - trues+randoms (T+R images)
  - trues+scatter+randoms (T+S+R images).
  - subtraction of T images from T+S images (S images)
  - subtraction of T images from T+R images (R images)

\

System 1, CW1400ps

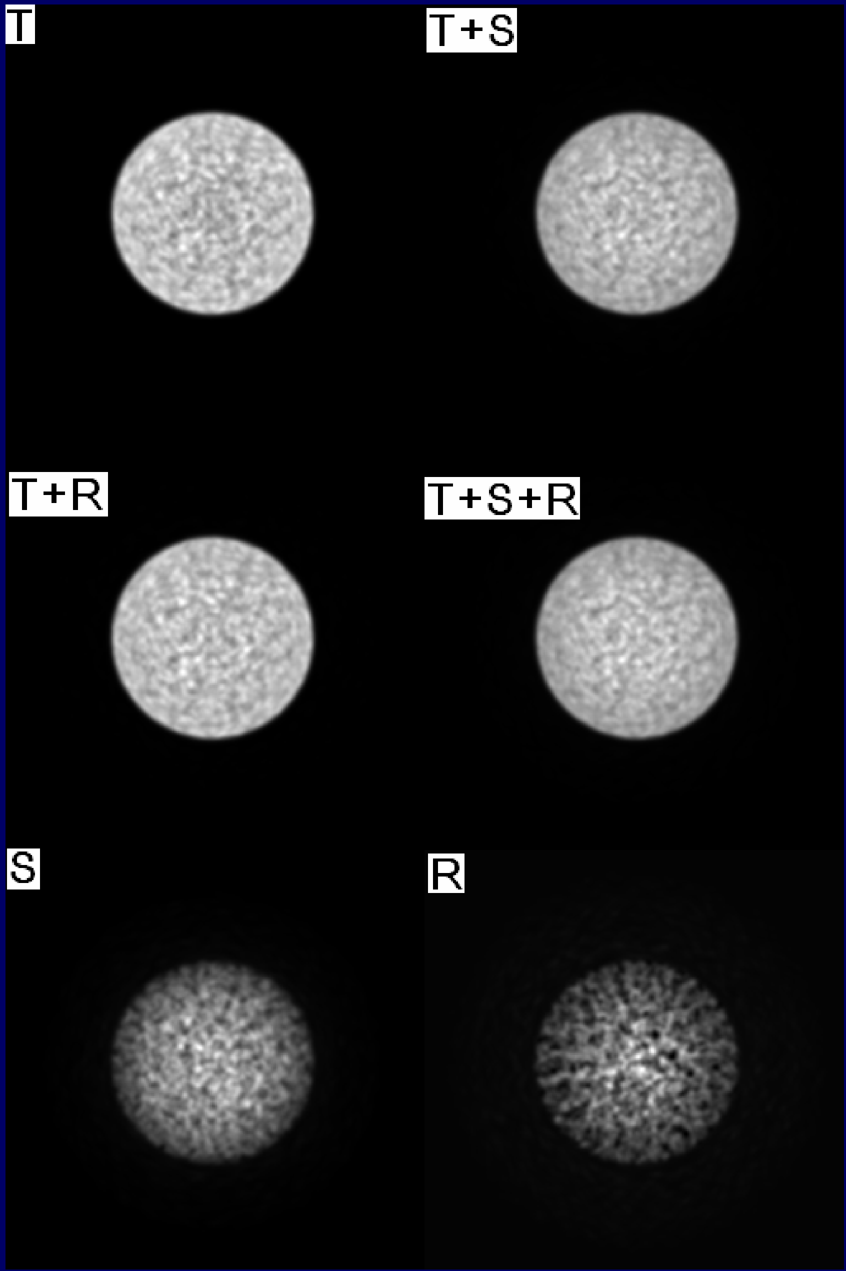

System 1, CW2000ps

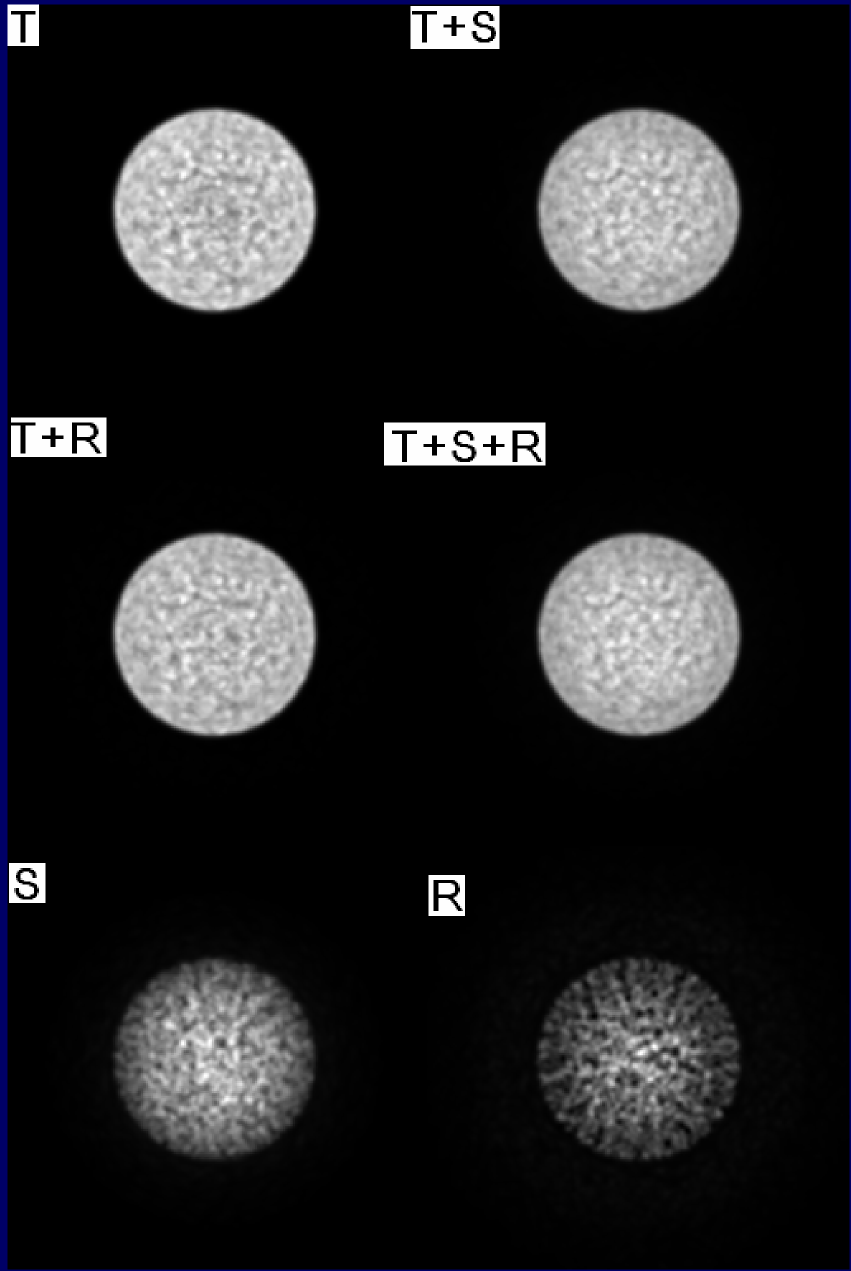

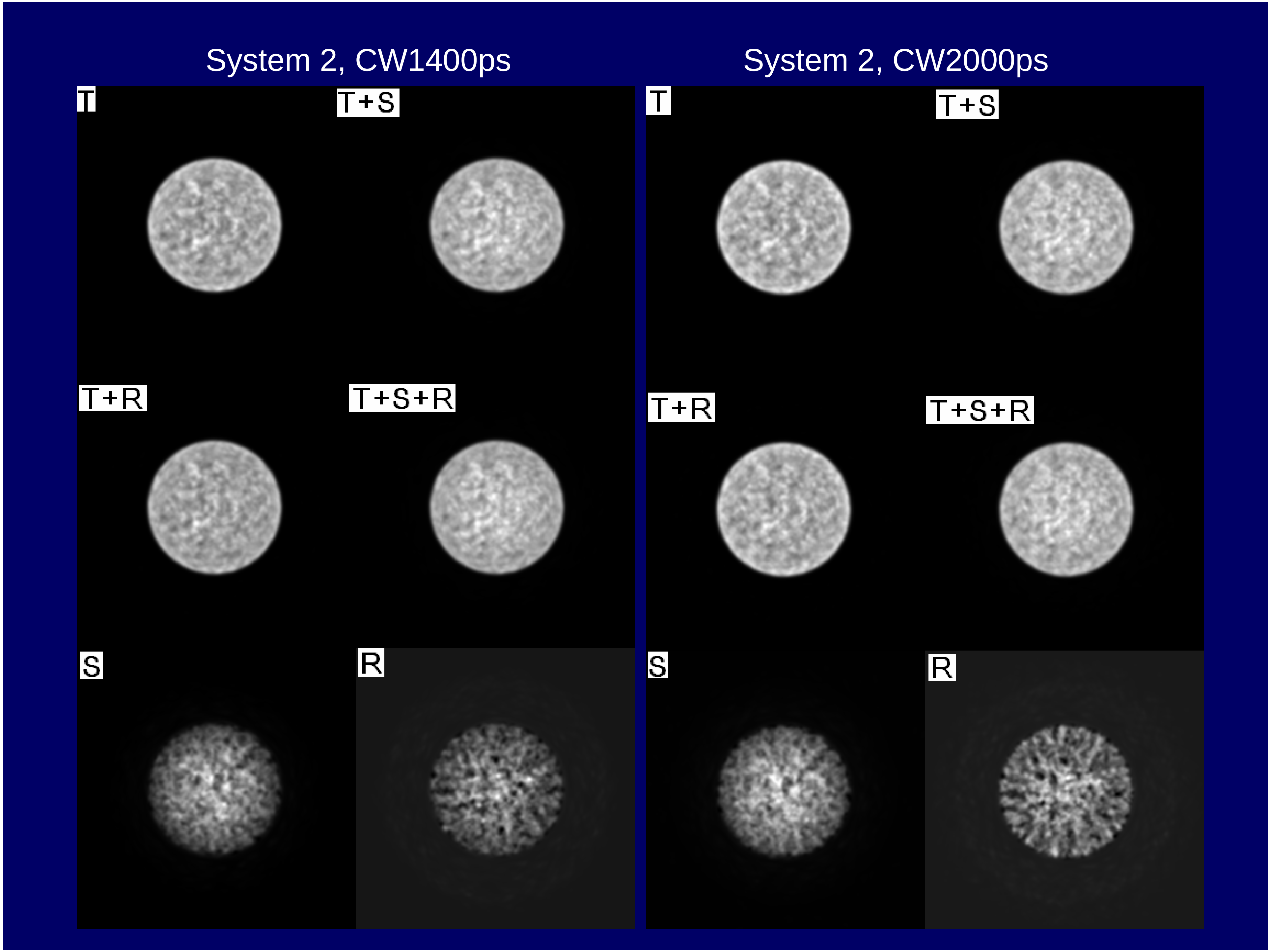
System 2, CW1400ps
System 2, CW2000ps
T
T+S
T+R
T+S+R
S
R
T
T+S
T+R
T+S+R
S
R

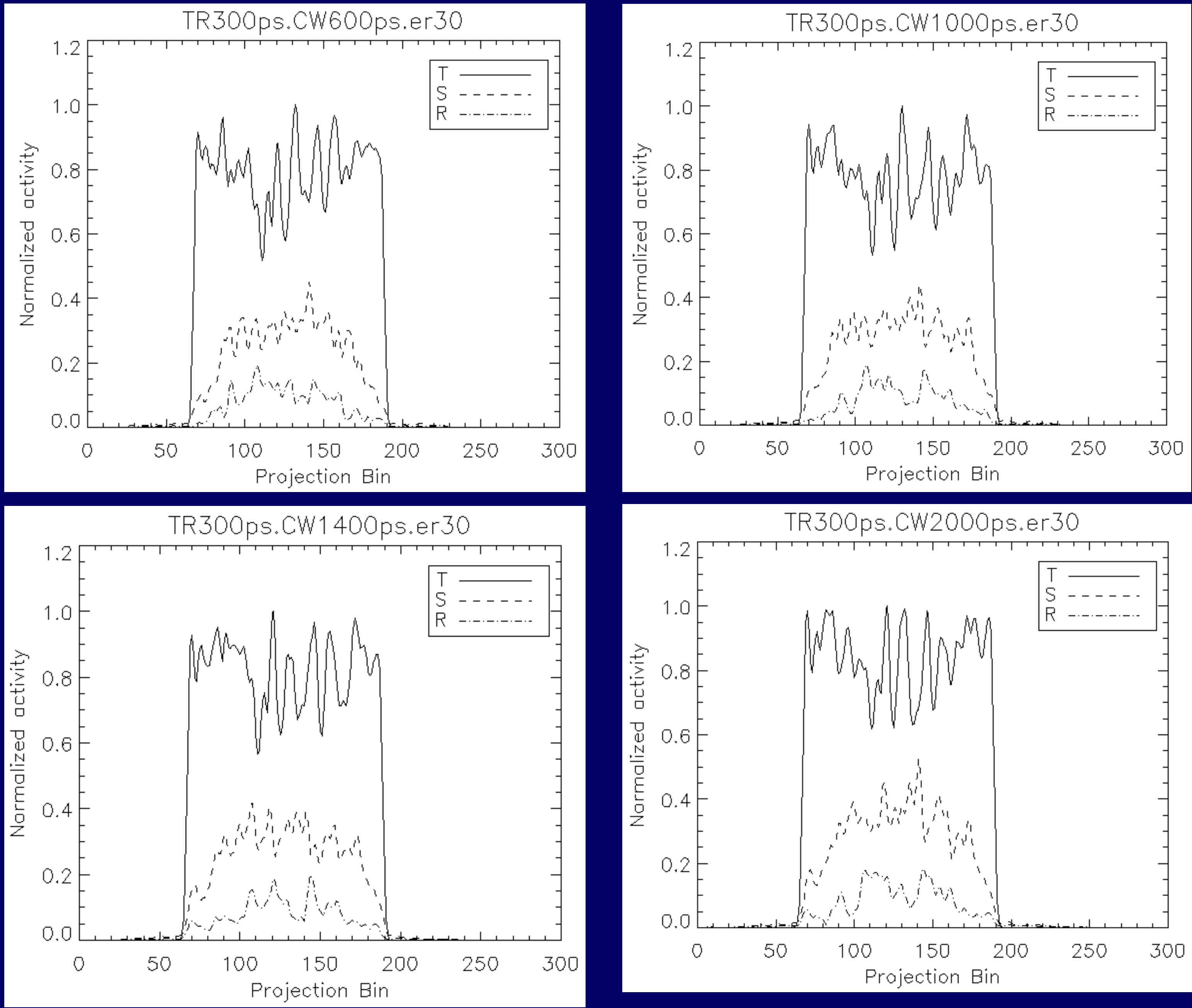

Central intensity profiles of images obtained with System 1

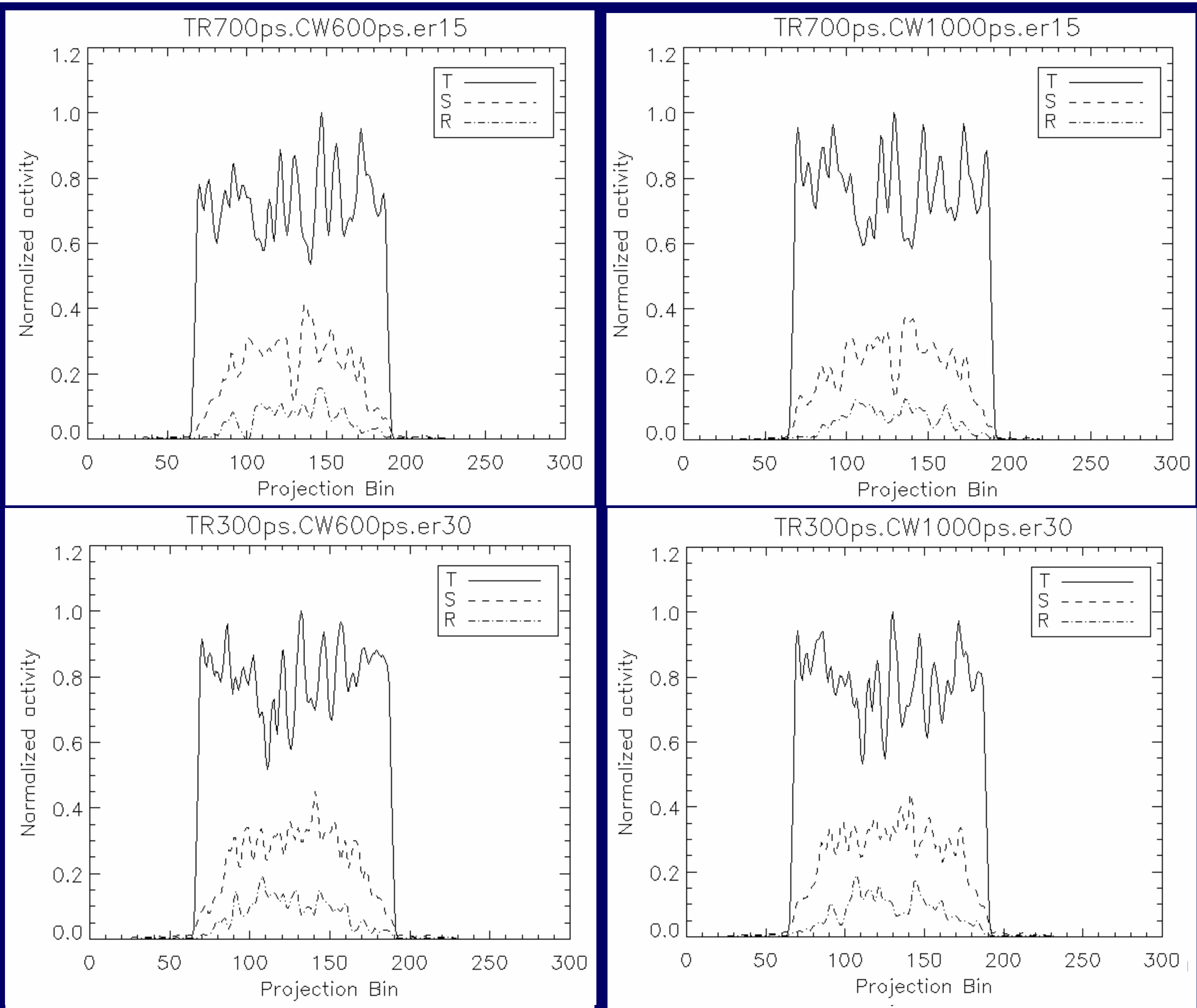

TR700ps.CW600ps.er15
TR700ps.CW1000ps.er15
TR300ps.CW600ps.er30
TR300ps.CW1000ps.er30
T
S
R
Normalized activity
Projection Bin
0.0
0.2
0.4
0.6
0.8
1.0
1.2
0
50
100
150
200
250
300

CW	600 ps		1 ns		1.4 ns		2 ns	
system	better-T_r	better-E_r	better-T_r	better-E_r	better-T_r	better-E_r	better-T_r	better-E_r
T	1.84	1.62	1.86	1.63	1.88	1.67	1.87	1.59
T+S	1.82	1.47	1.81	1.46	1.76	1.47	1.79	1.43
T+R	2.28	1.74	2.17	1.73	2.17	1.76	2.23	1.67
T+S+R	2.35	1.74	2.40	1.77	2.36	1.82	2.39	1.75

Table 2: Gains in the ROI SNR achieved by two systems (better-T_r system: E_r = 30%, T_r = 300 ps; better-E_r system: E_r = 10%, T_r = 700 ps) when employing various CWs and reconstructed by using the EM algorithm. The data either contains true events only (T), true and scatter (T+S), true and randoms (T+R), or all event types (T+S+R). Generally, the best SNR gain was obtained with the better-T_r system when employing 1 ns CW.

Single-Photon Emission Computed Tomography (SPECT)

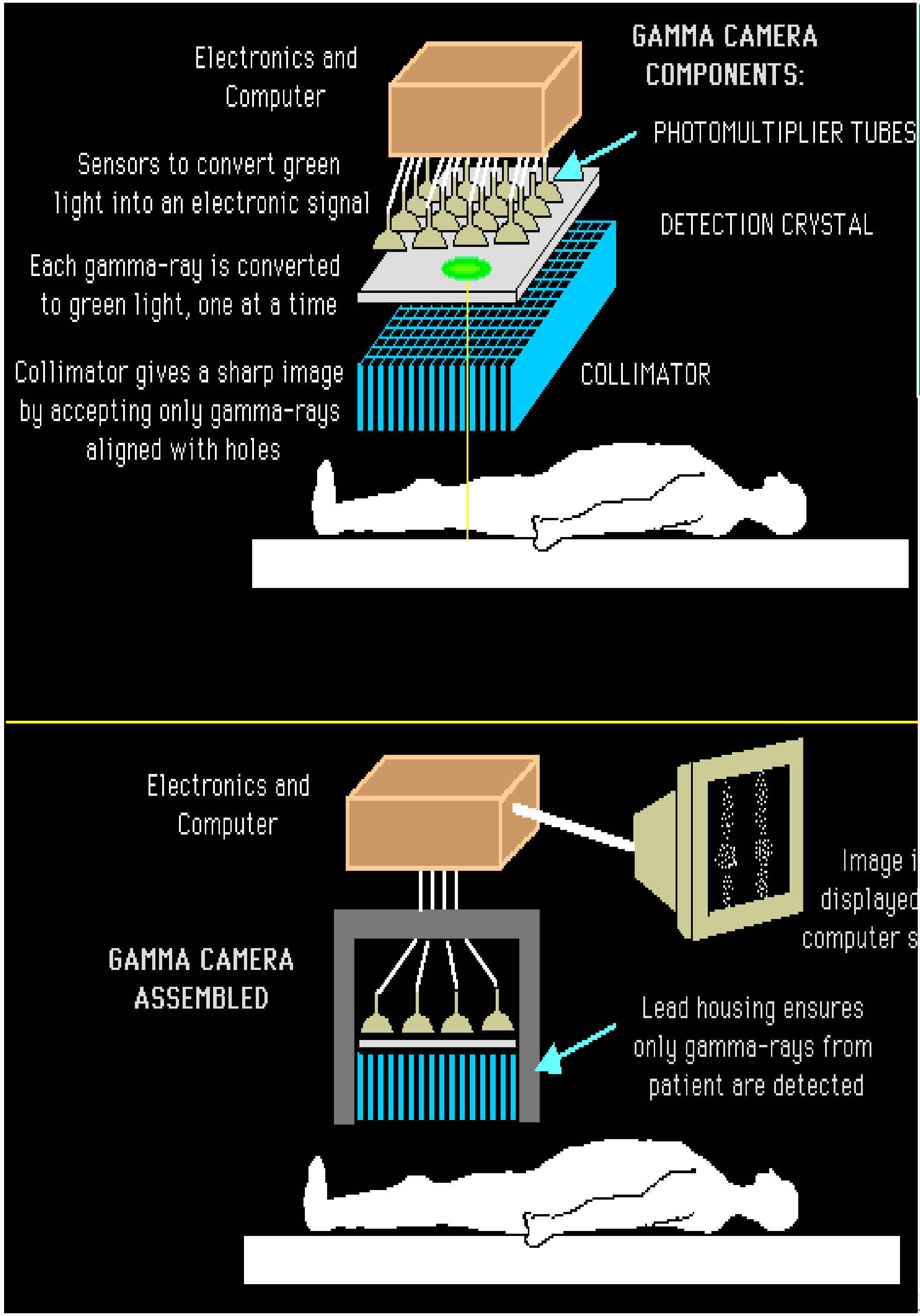

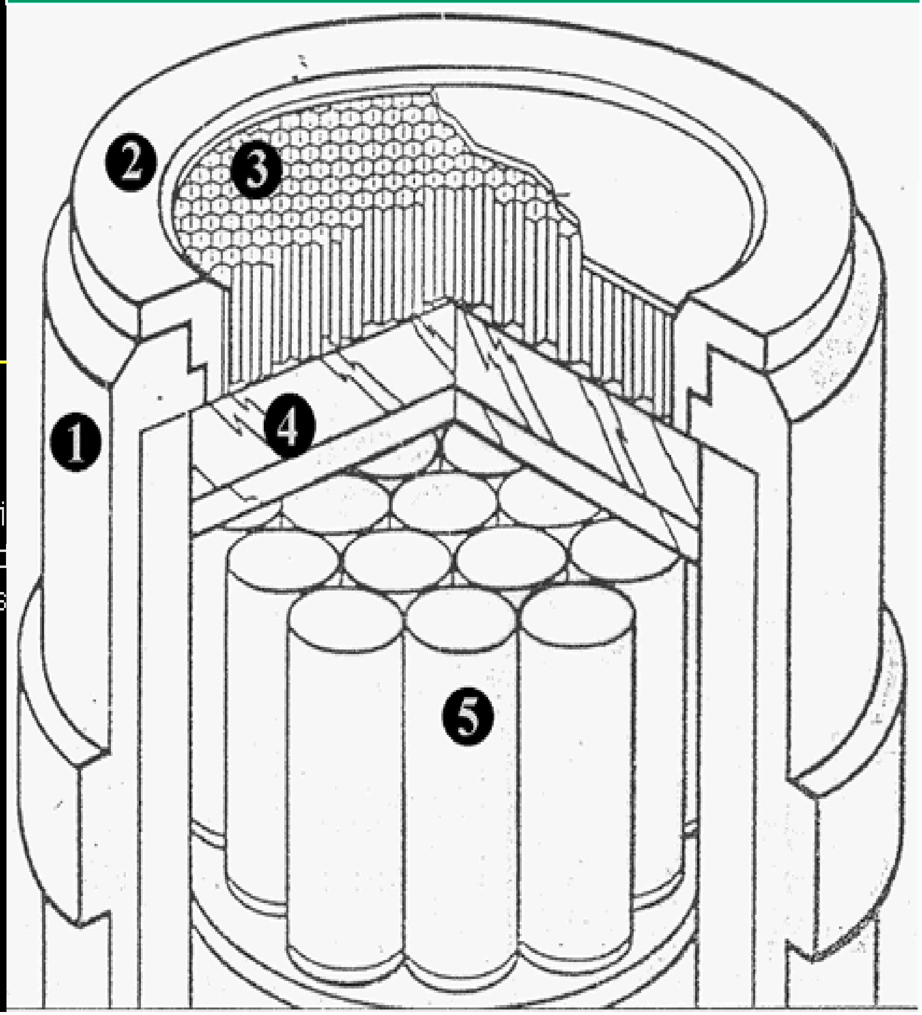

Single-Photon Radionuclides

Name	$T_{1/2}$	γ or x-ray (keV)	abundance
^{133}Xe	5.3 days	81	0.38
^{99m}Tc	6.0 hrs	140	0.89
^{111}In	2.8 days	171	0.90
		245	0.94
^{123}I	13 hrs	159	0.99
^{67}Ga	3.3 days	92	0.38
		184	0.23
		300	0.16

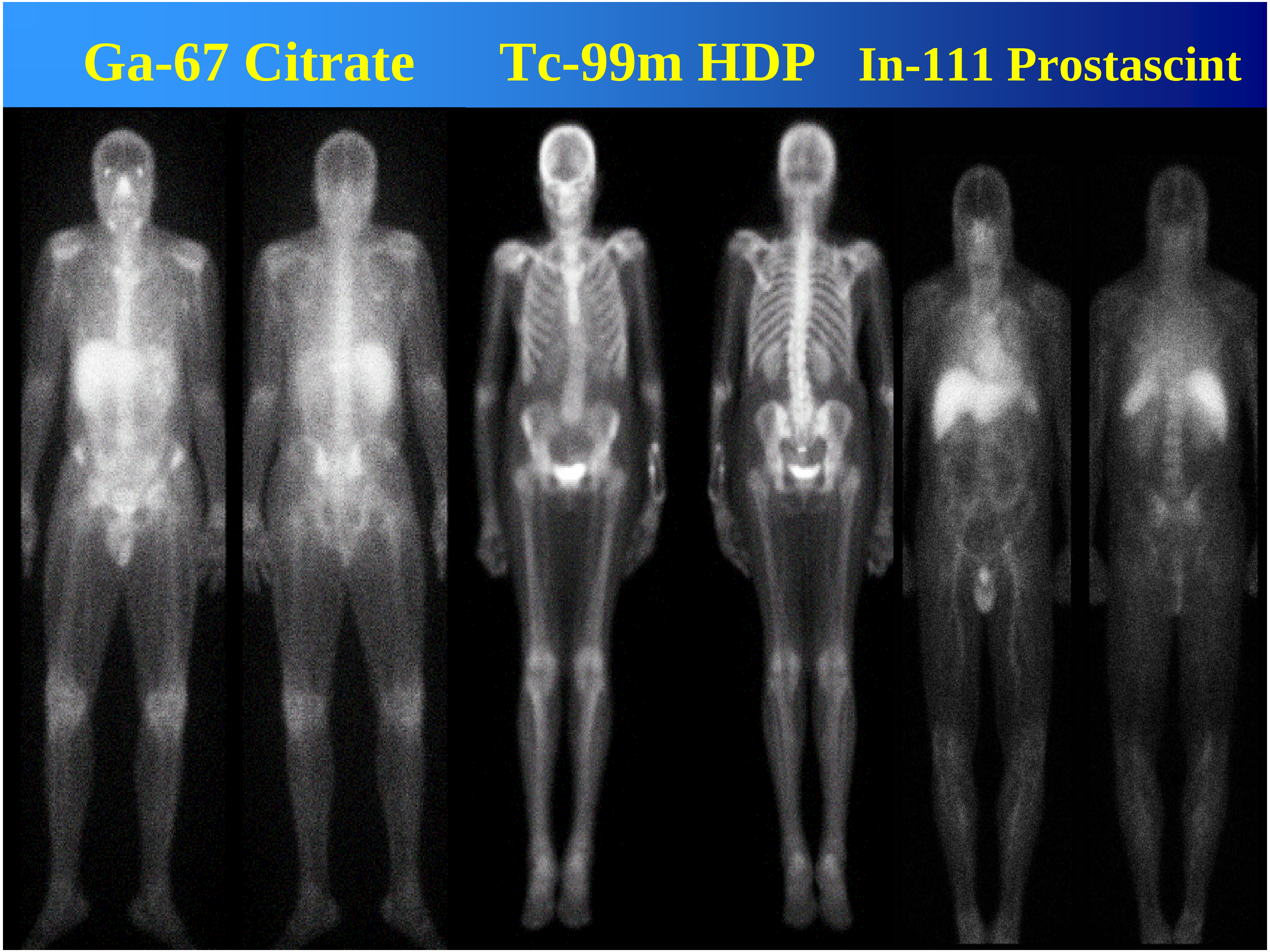
Ga-67 Citrate
Tc-99m HDP
In-111 Prostascint

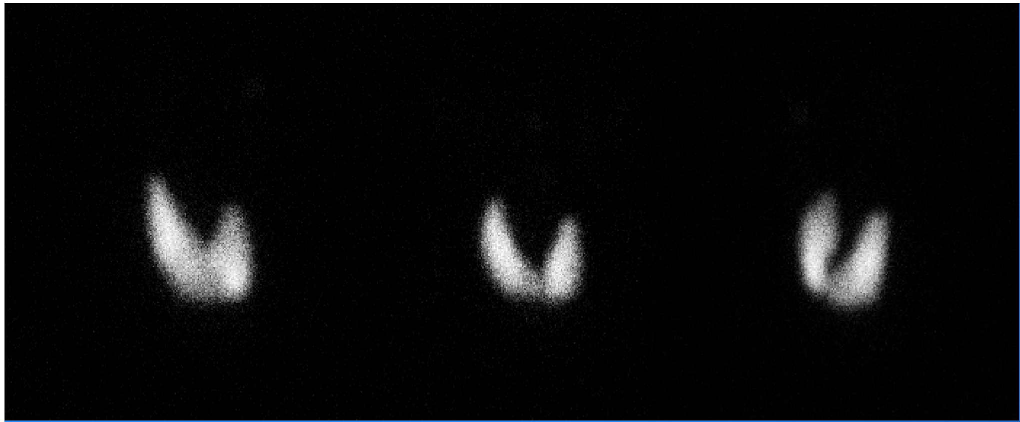

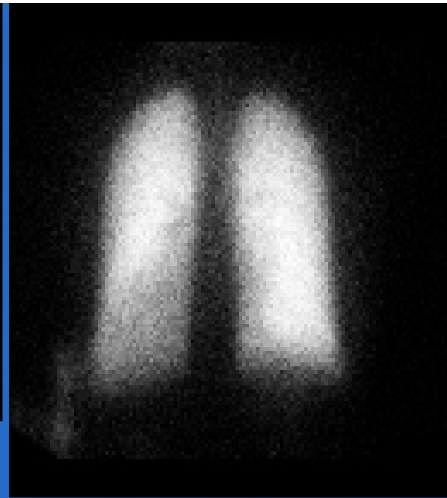

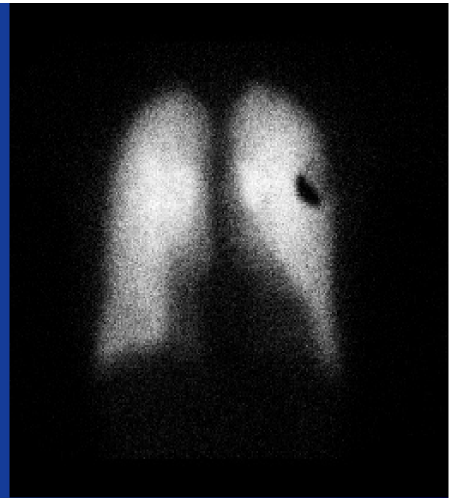

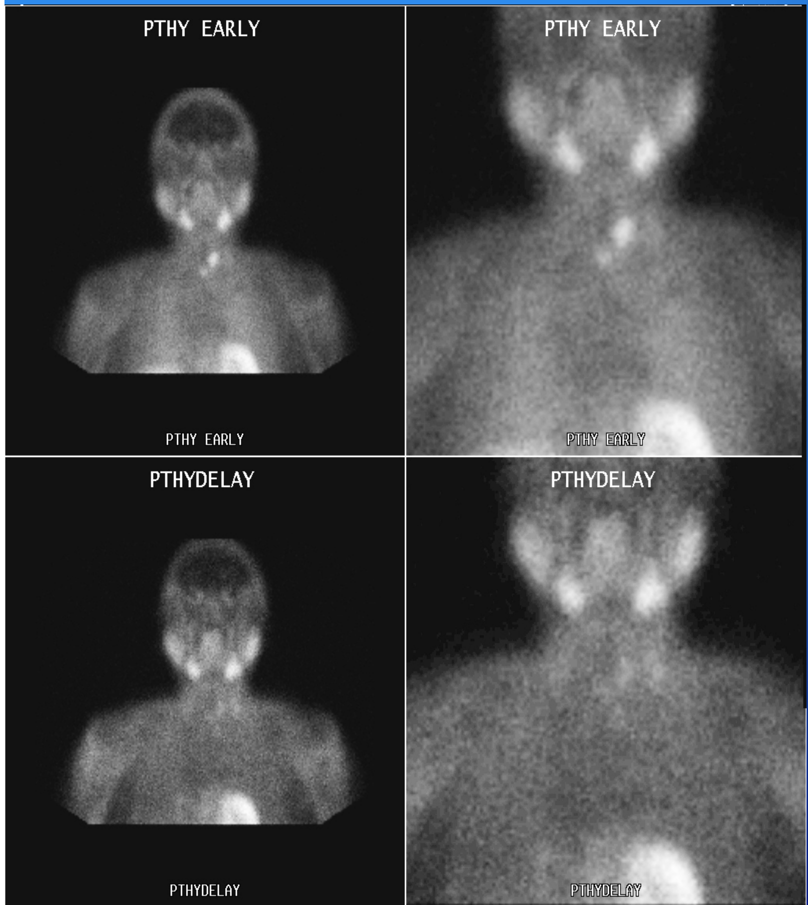
PTHY EARLY
PTHY EARLY
PTHY EARLY
PTHY EARLY
PTHYDELAY
PTHYDELAY
PTHYDELAY
PTHYDELAY

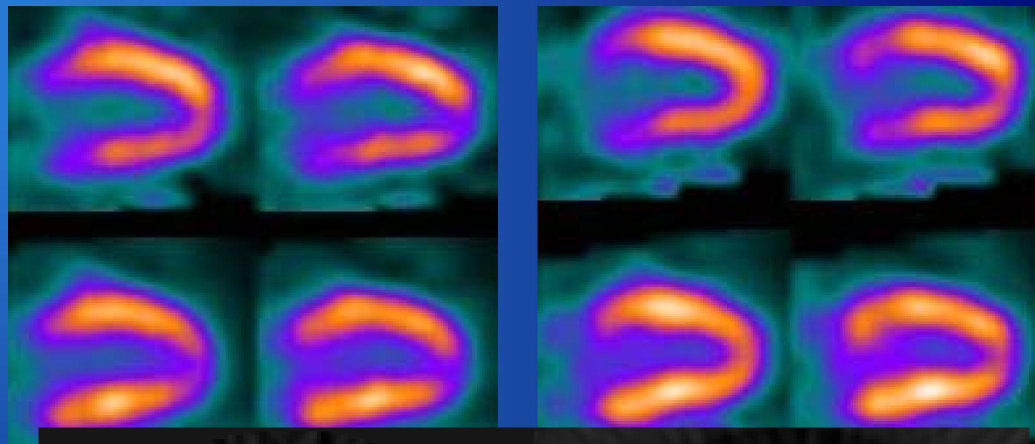

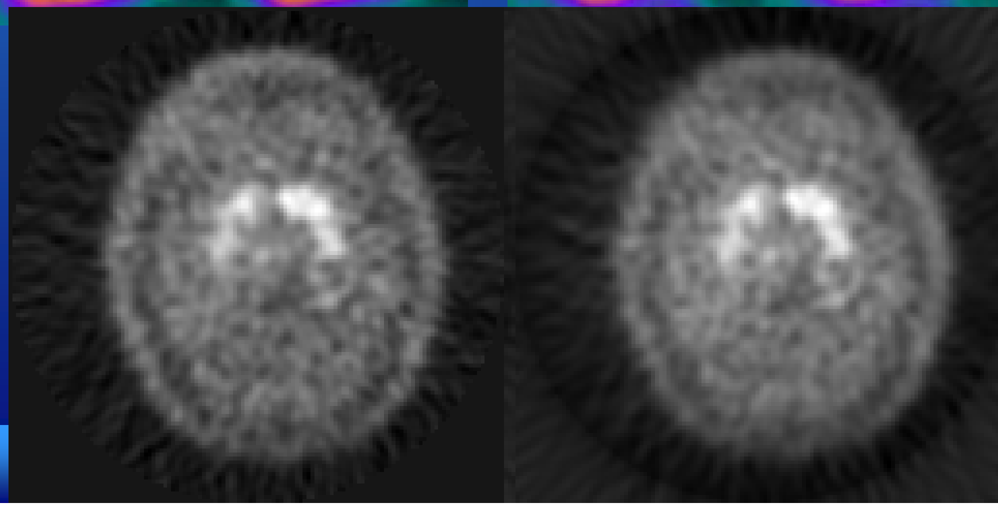

Triple-Head SPECT Scanner

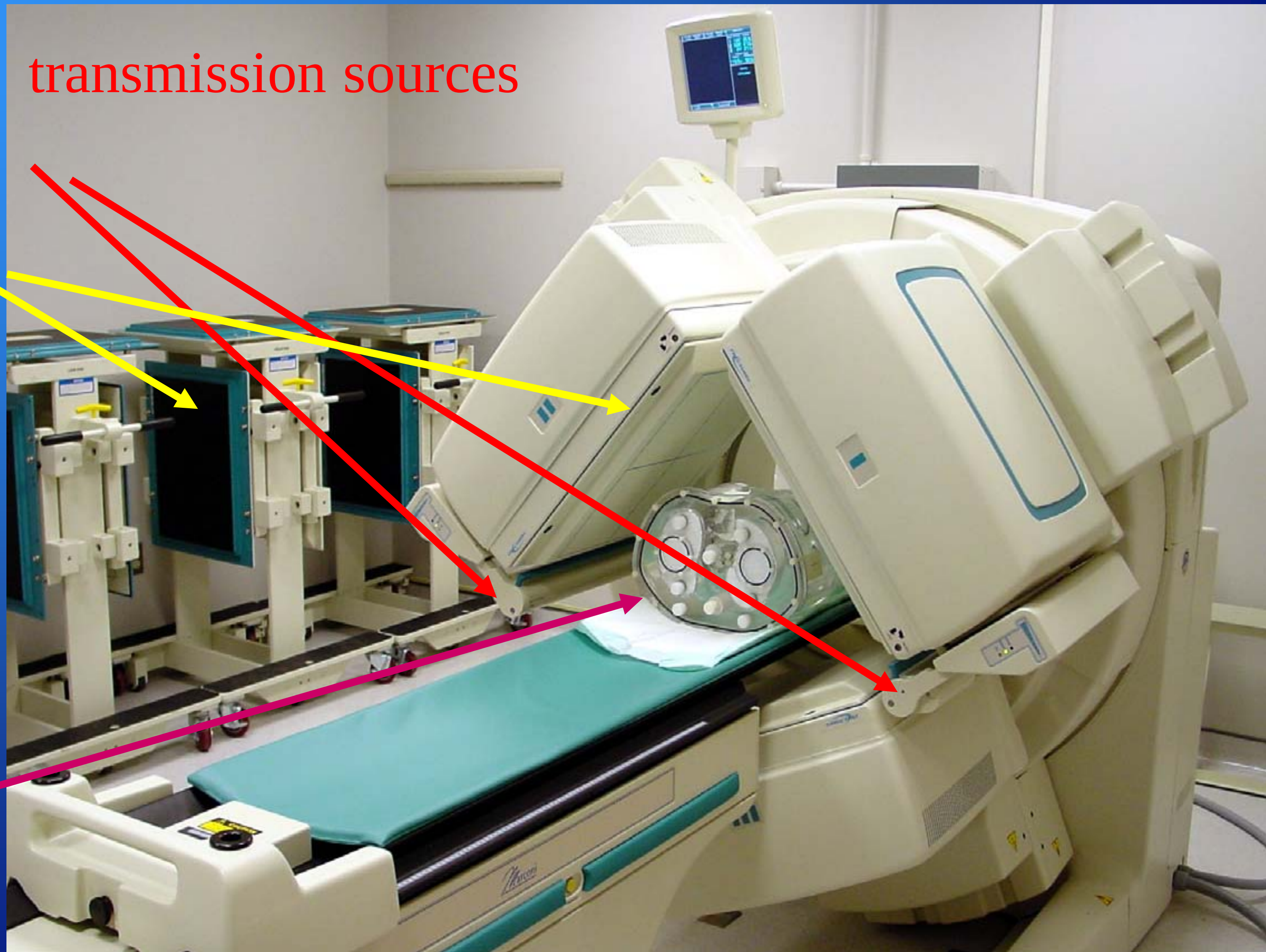

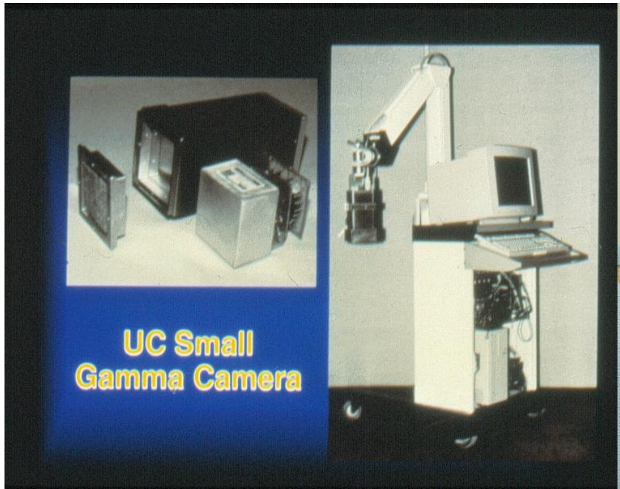
UC Small
Gamma Camera

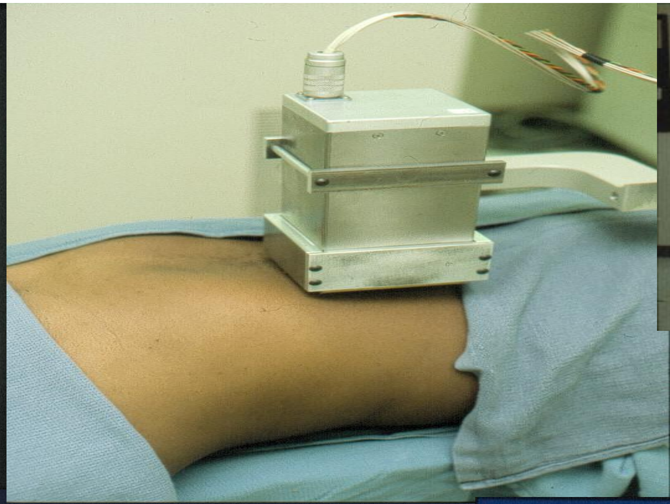

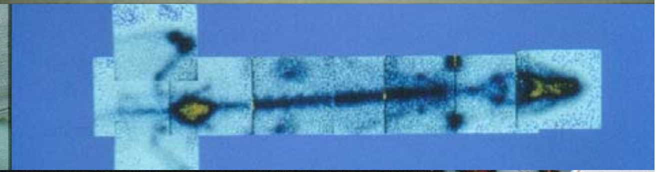

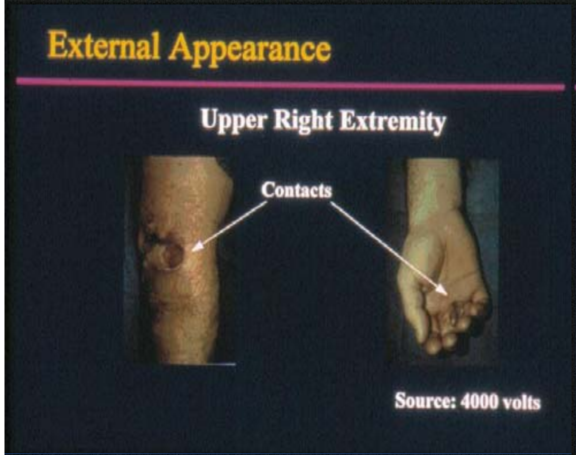
External Appearance
Upper Right Extremity
Contacts
Source: 4000 volts

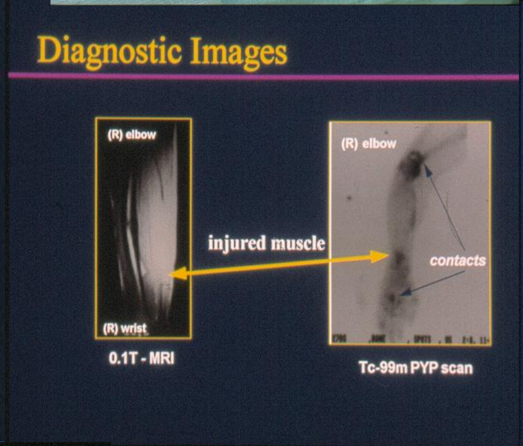
Diagnostic Images
(R) elbow
(R) wrist
0.1T - MRI
injured muscle
(R) elbow
contacts
Tc-99m PYP scan

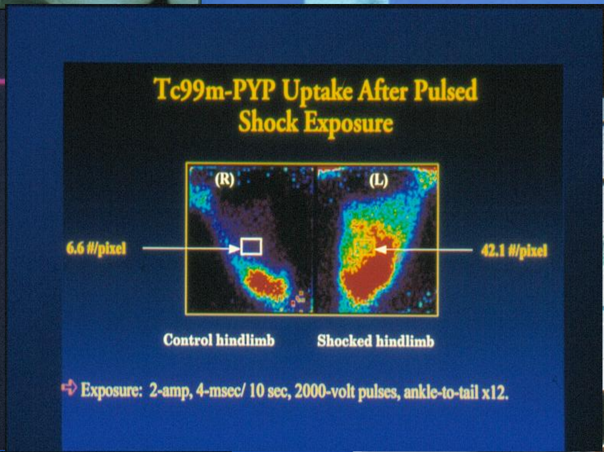
Tc99m-PYP Uptake After Pulsed
Shock Exposure
(R)
(L)
6.6 #/pixel
42.1 #/pixel
Control hindlimb
Shocked hindlimb
Exposure: 2-amp, 4-msec/ 10 sec, 2000-volt pulses, ankle-to-tail x12.

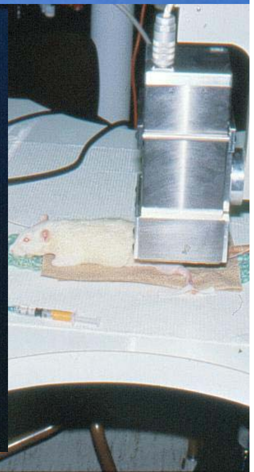

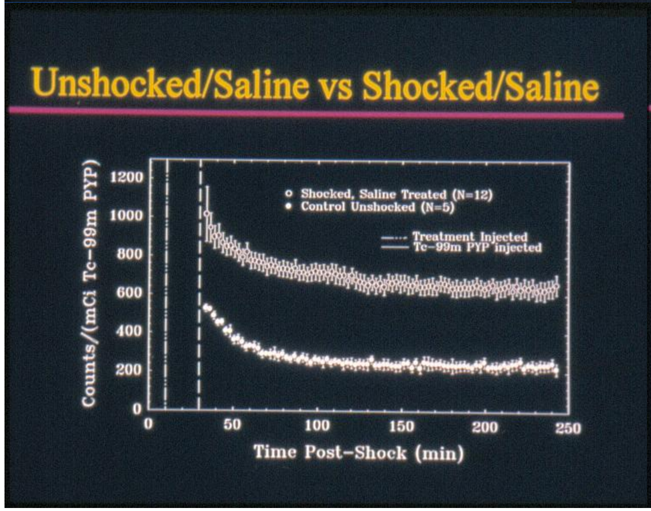
Unshocked/Saline vs Shocked/Saline
Counts/(mCi Tc-99m PYP)
Time Post-Shock (min)
Shocked, Saline Treated (N=12)
Control Unshocked (N=5)
Treatment Injected
Tc-99m PYP injected
0
200
400
600
800
1000
1200
50
100
150
200
250

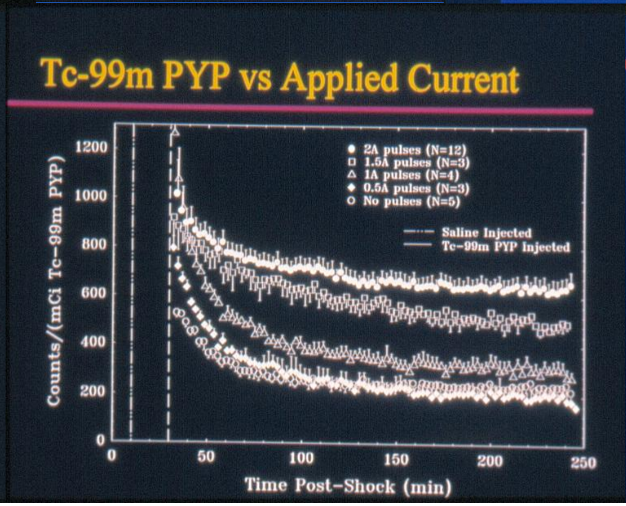
Tc-99m PYP vs Applied Current
Counts/(mCi Tc-99m PYP)
Time Post-Shock (min)
2A pulses (N=12)
1.5A pulses (N=3)
1A pulses (N=4)
0.5A pulses (N=3)
No pulses (N=5)
Saline Injected
Tc-99m PYP Injected
0
200
400
600
800
1000
1200
50
100
150
200
250

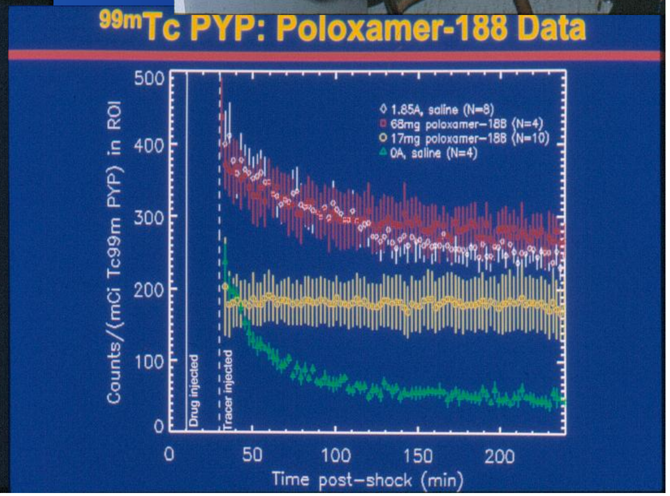
99mTc PYP: Poloxamer-188 Data
Counts/(mCi Tc99m PYP) in ROI
Time post-shock (min)
1.85A, saline (N=8)
68mg poloxamer-188 (N=4)
17mg poloxamer-188 (N=10)
0A, saline (N=4)
Drug injected
Tracer injected
0
100
200
300
400
500
50
150
200

Super-Resolution Imaging (J. Meng, UIUC)
Single-Photon Emission Microscopy (SPEM)

A New Photon Sensor – Electron Multiplying Charge-coupled Devices

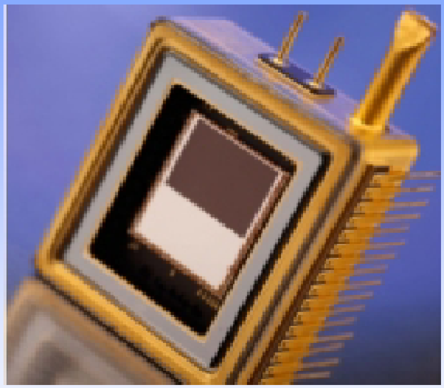

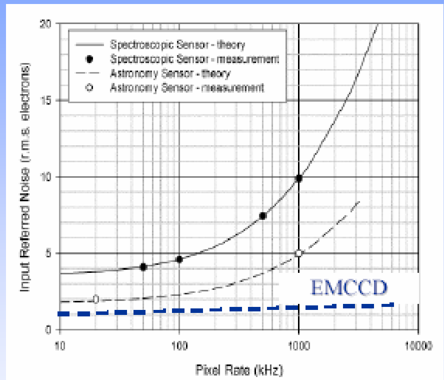

The Very-high Resolution Gamma Camera

Basic Configuration:

- Readout sensor: Electron Multiplying Charge Coupled Device (EMCCD).
- DM tube gain: 1 p.e. → ~60 photons
- Overall DM ratio: 6:1
- Overall detector active area: ~5x5 cm^2.
- Conversion material: CsI(Tl), Gadox or other scintillation material.
- Rely on light sharing between CCD pixels to achieve a very high spatial resolution (typically <60μm FWHM).
- Used with multiple micro-pinholes, typically 100μm diameter.

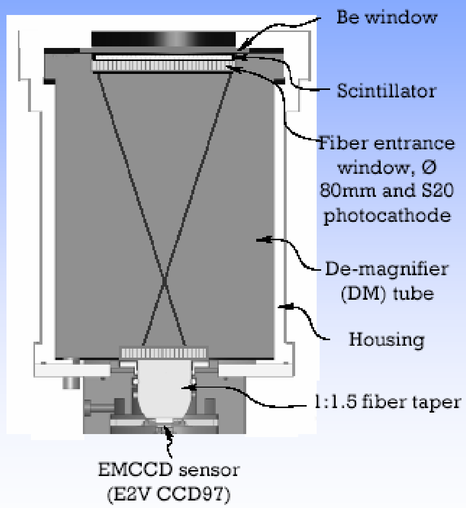

Measurements with Fiber Optic Coupling

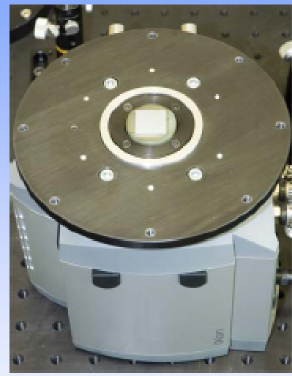

EMCCD camera with fiber taper and columnar-grown CsI(Tl) scintillator

- EMCCD sensor: E2V L3Vision CCD97, back illuminated frame transfer device.
- CCD Resolution: 512×512 pixels, 16×16 $micron^2$.
- Maximum readout speed: 10MHz, ~30 f/s at full frame.
- Actual optical pixel size: 24×24μm^2 (with 1.5:1 fiber taper).
- TE cooling to -40°C.
- Typical operating EM gain: ~300.
- Scintillator used: columnar CsI(Tl) phosphor (Hamamatsu ACS HL,

Spatial Resolution for Planar Imaging Case

Experimental Setup

- Detector active area: ~5×5cm^2
- Collimator: single pinhole aperture.
- Pinhole diameter: 100μm.
- Source-to-pinhole distance: ~2cm.
- Pinhole-to-detector distance: ~2cm.
- Reconstruction with standard MLEM.
- Source plane: 512×512 pixels, pixel size: 32×32μm^2.

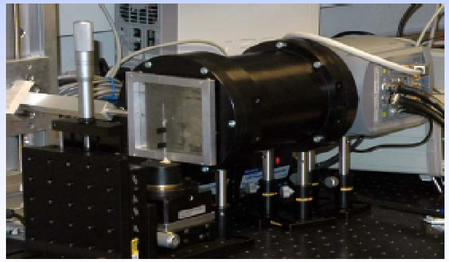

Super-Resolution Imaging Single-Photon Emission Microscopy (SPEM)

Measured Intrinsic Spatial Resolution

EMCCD Binning	Readout Frame Rate (fps)	Optical Pixel Size (μm)	FWHM (μm)	FWTM (μm)
EMCCD only	32	24	35	--
512×512	32	96	60	123
256×256	54	192	92	190
128×128	95	384	109	227

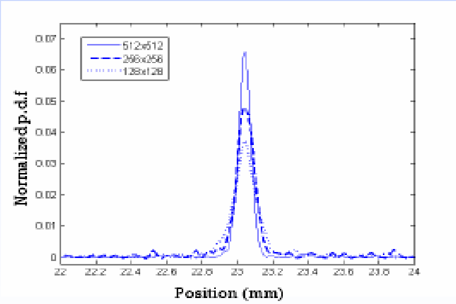

Measured line-spread functions with different binning

Reconstructed Mouse Thyroid Image

Total activity: 500μCi.
Thyroid uptake: ~50μCi

Measuring time: ~1 hours
Pinhole diameter: 100 μ

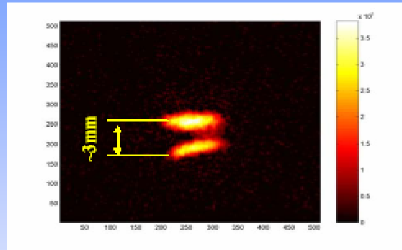

100μm pinhole

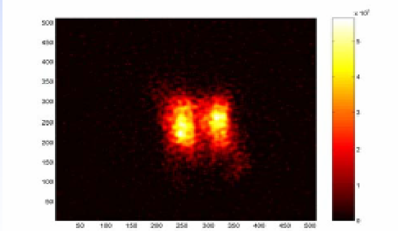

300μm pinhole

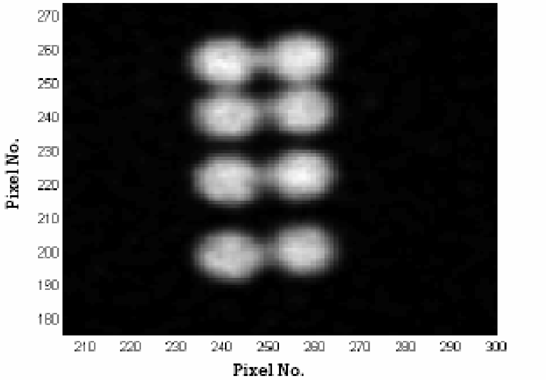

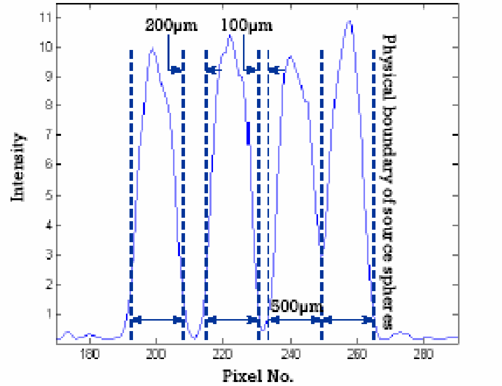

Reconstruction of multiple sphere sources

1-d profile of cutting through the four spheres on the right hand side

Measured spatial resolution <80μm !

Super-Resolution Imaging
Single-Photon Emission Microscopy (SPEM)

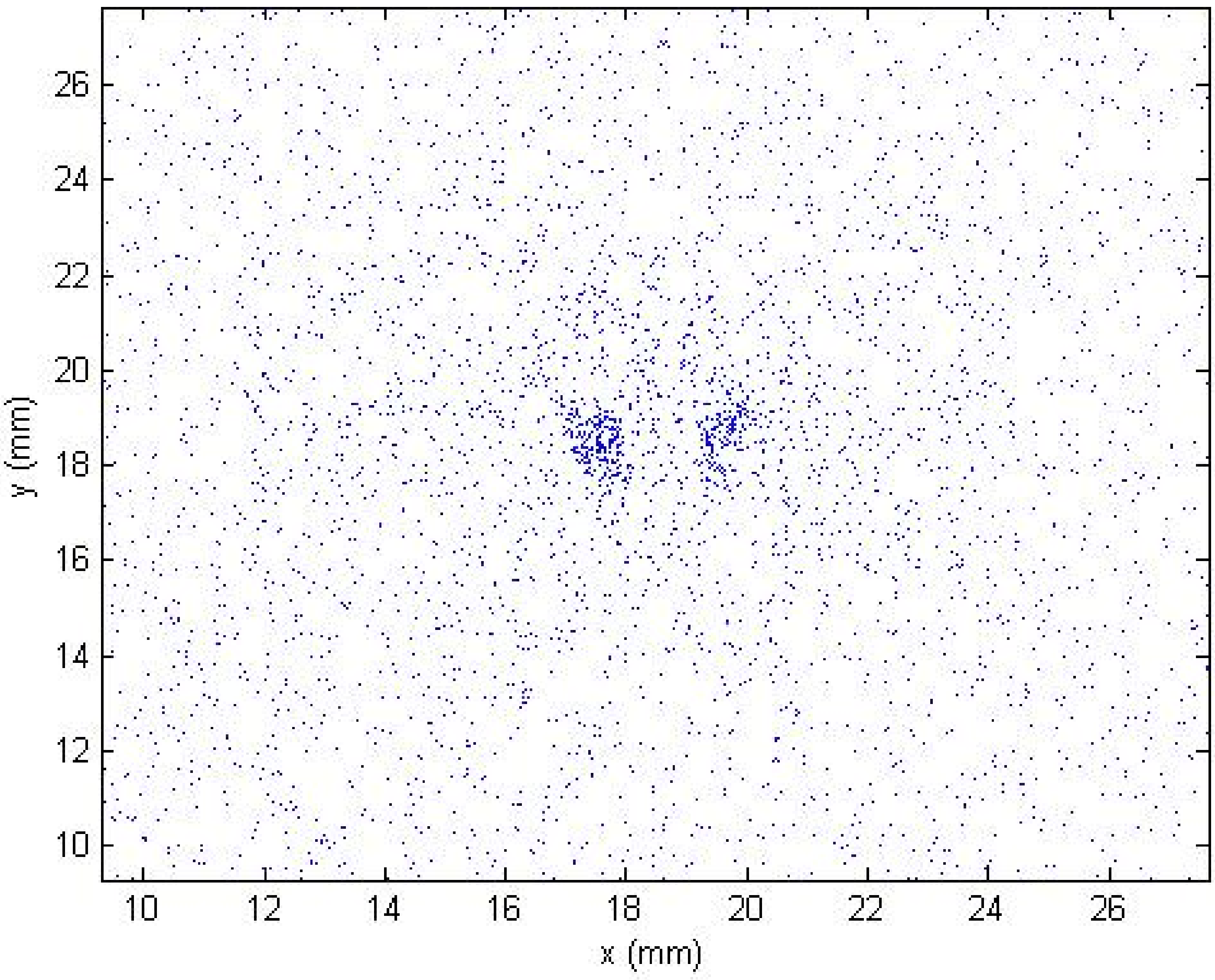

Integrative SPEM and CT

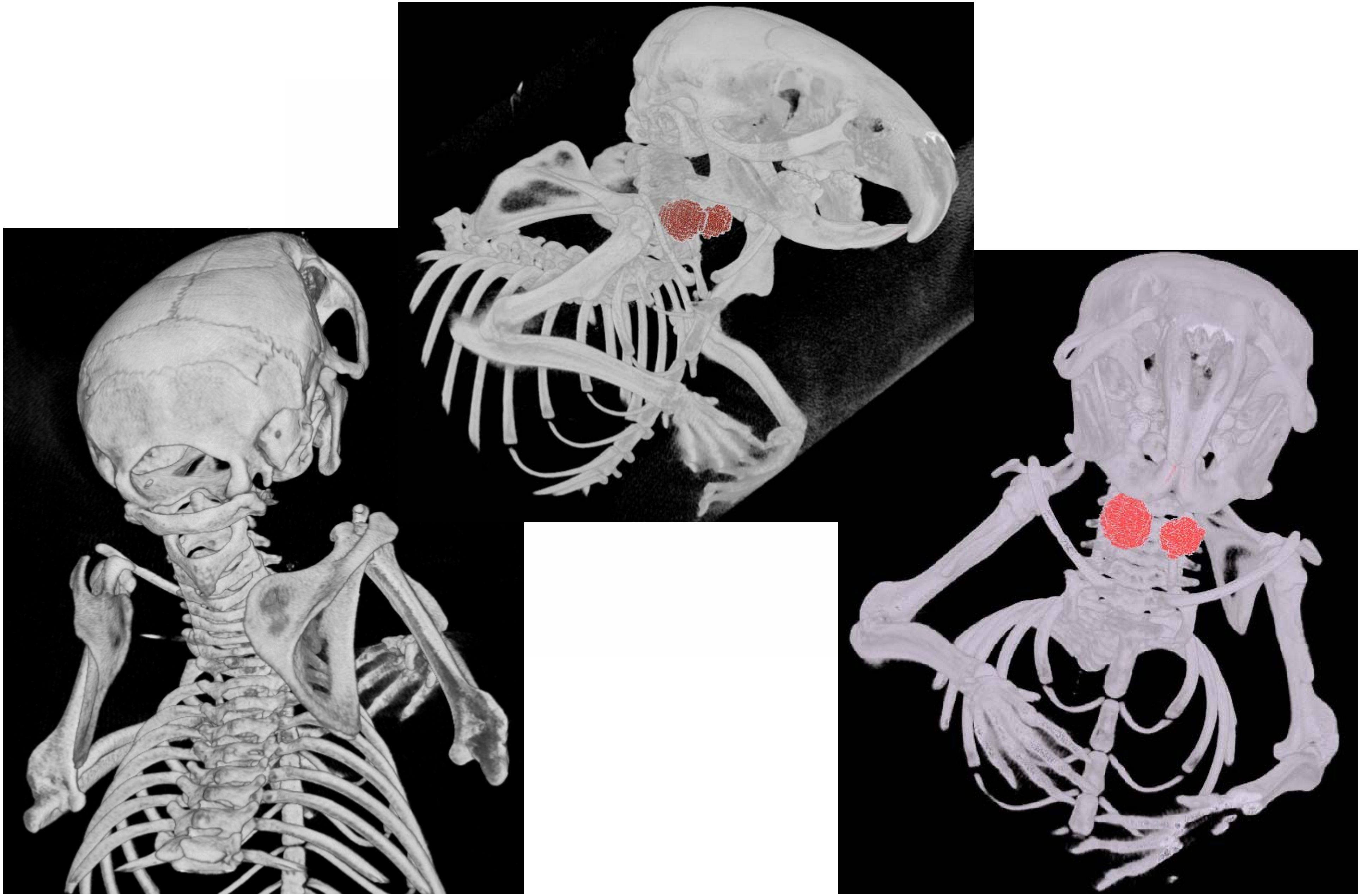

The Best Existing Technology

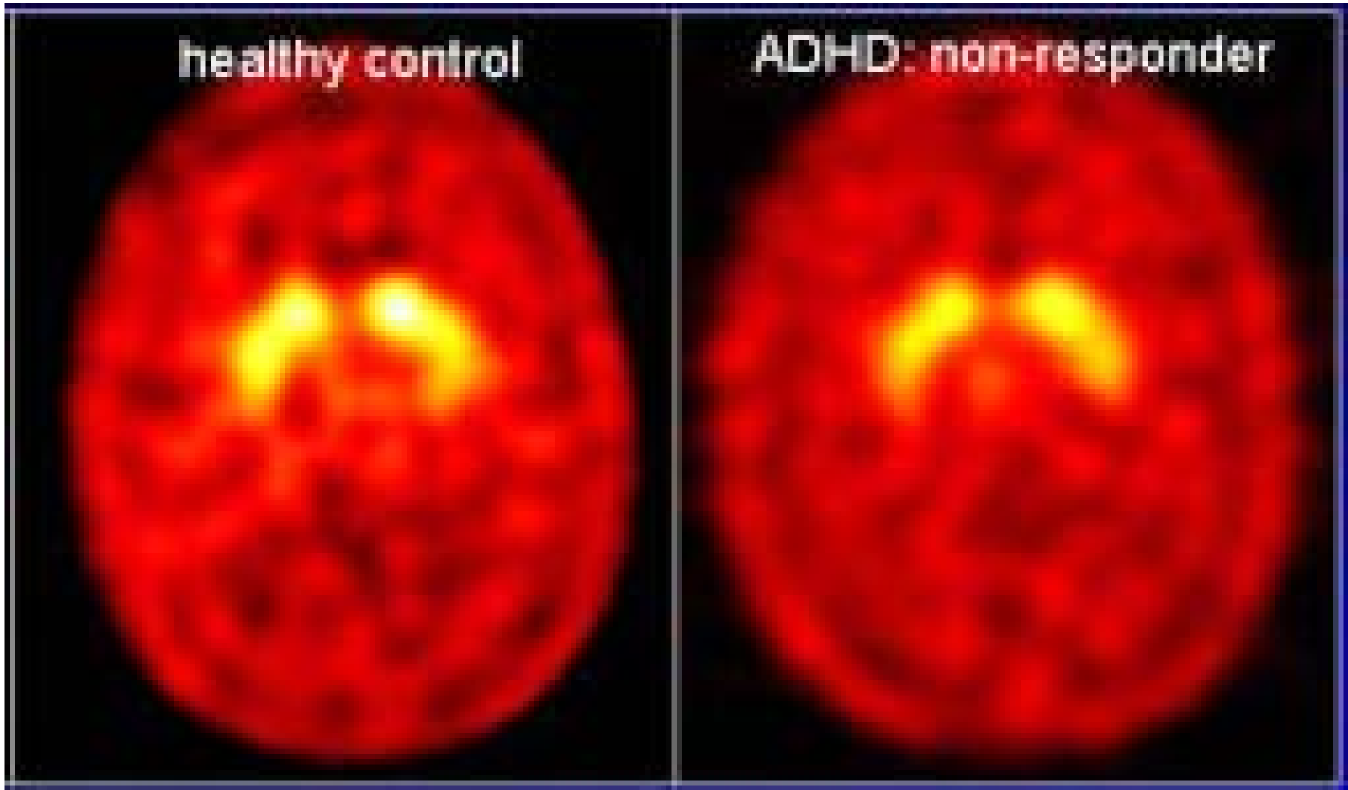

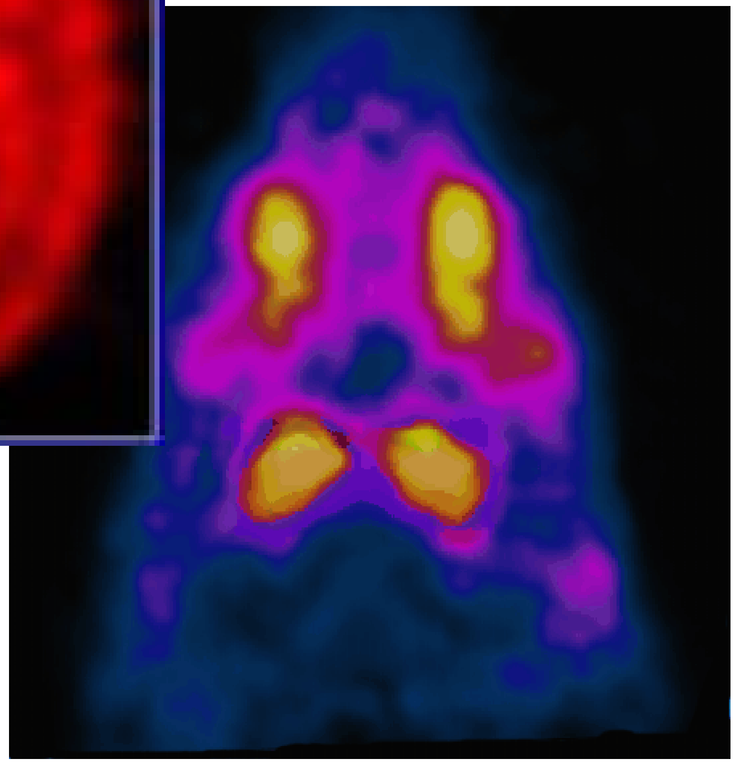

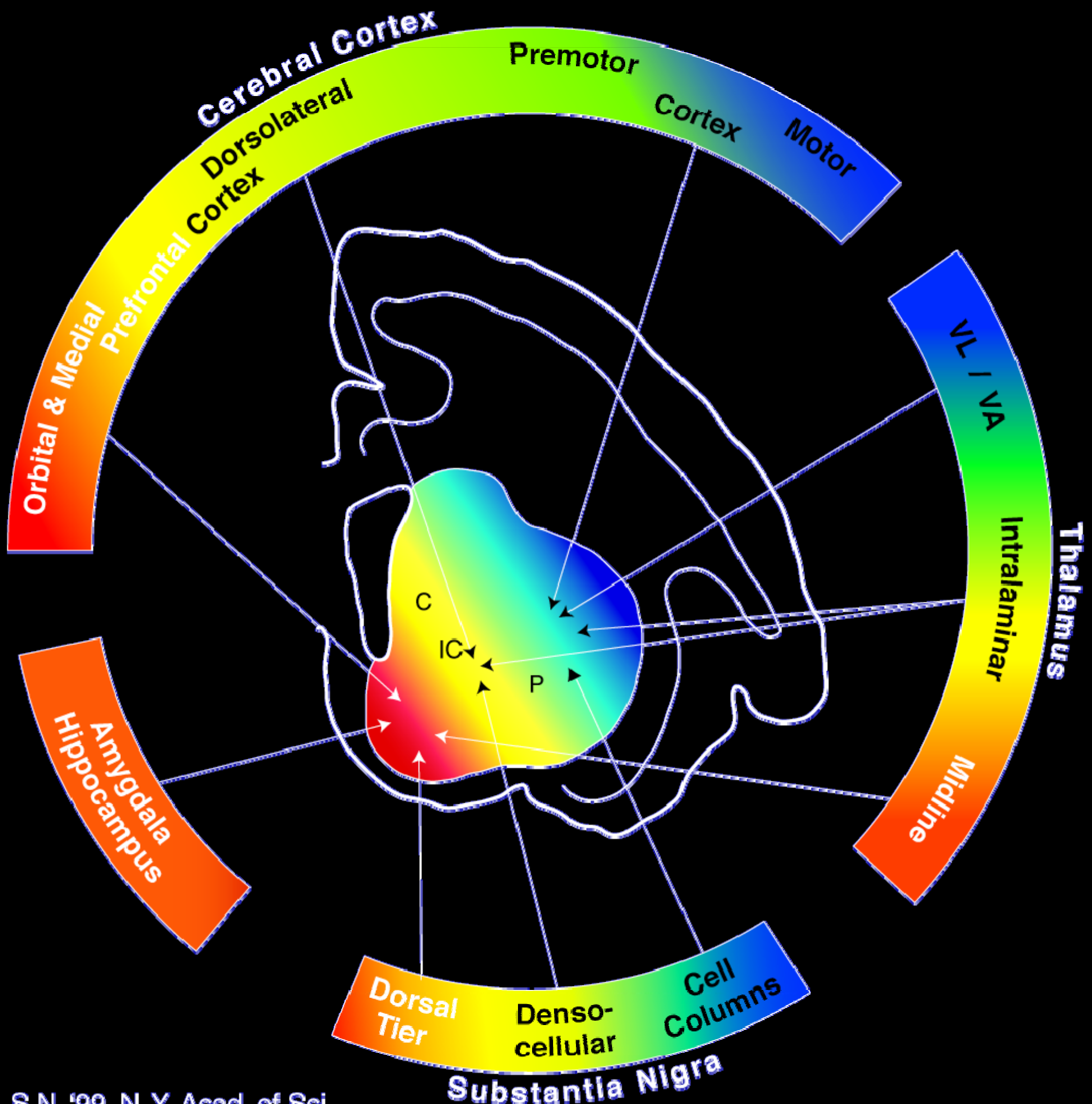

Haber, S.N. '99. N. Y. Acad. of Sci.

Super-Resolution Imaging
Single-Photon Emission Microscopy (SPEM)

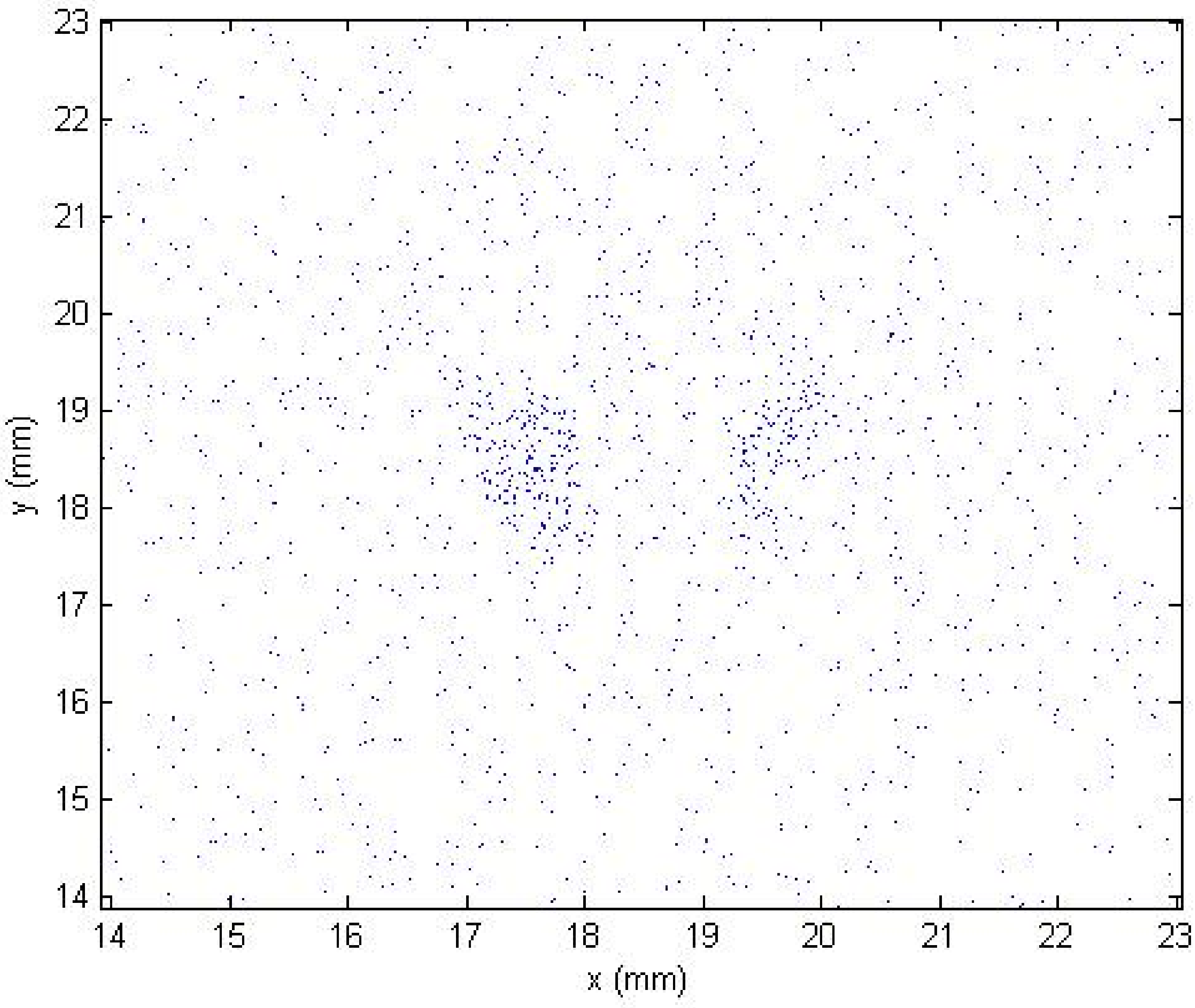

Few-View Image Reconstruction (Using GATE)

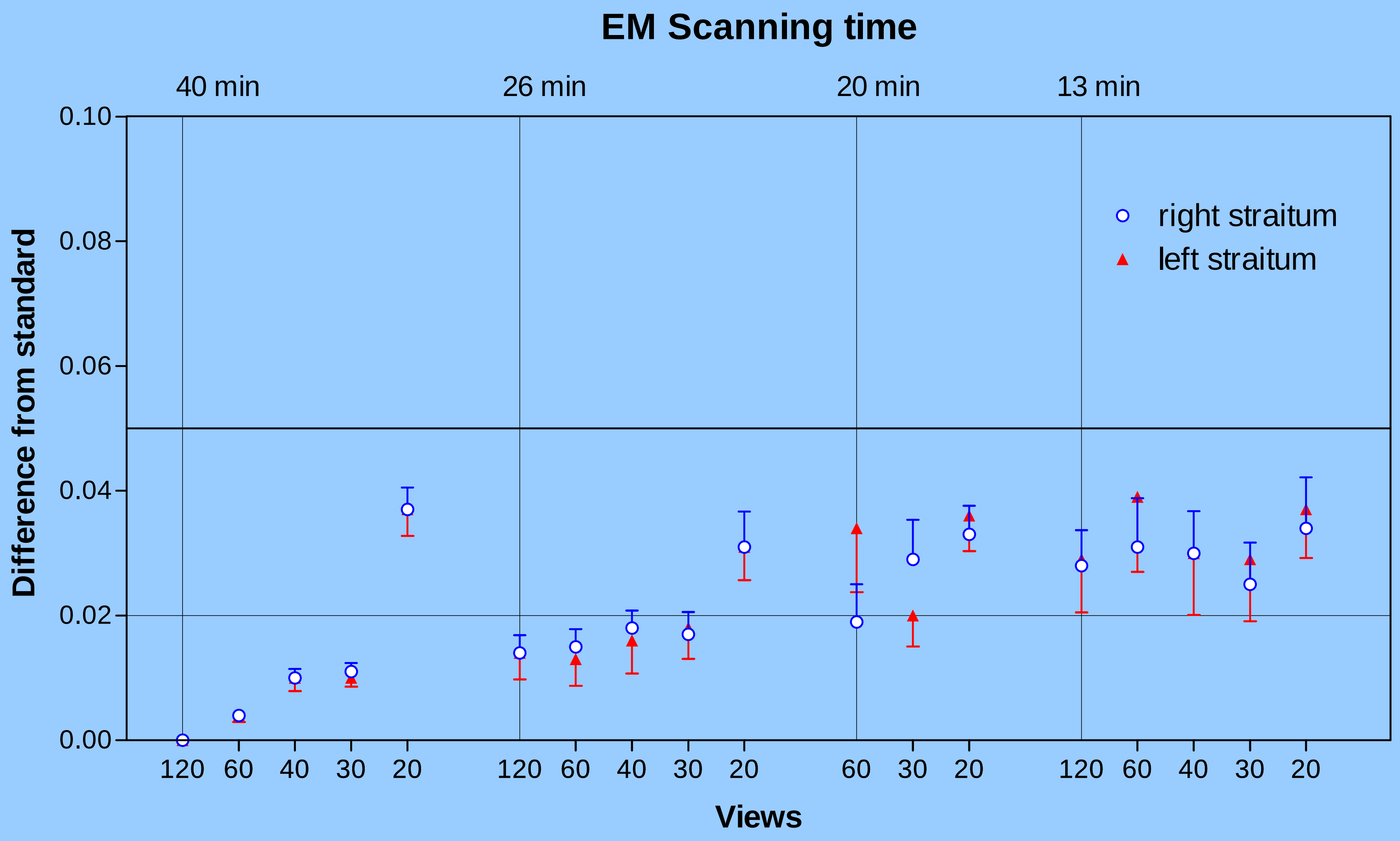

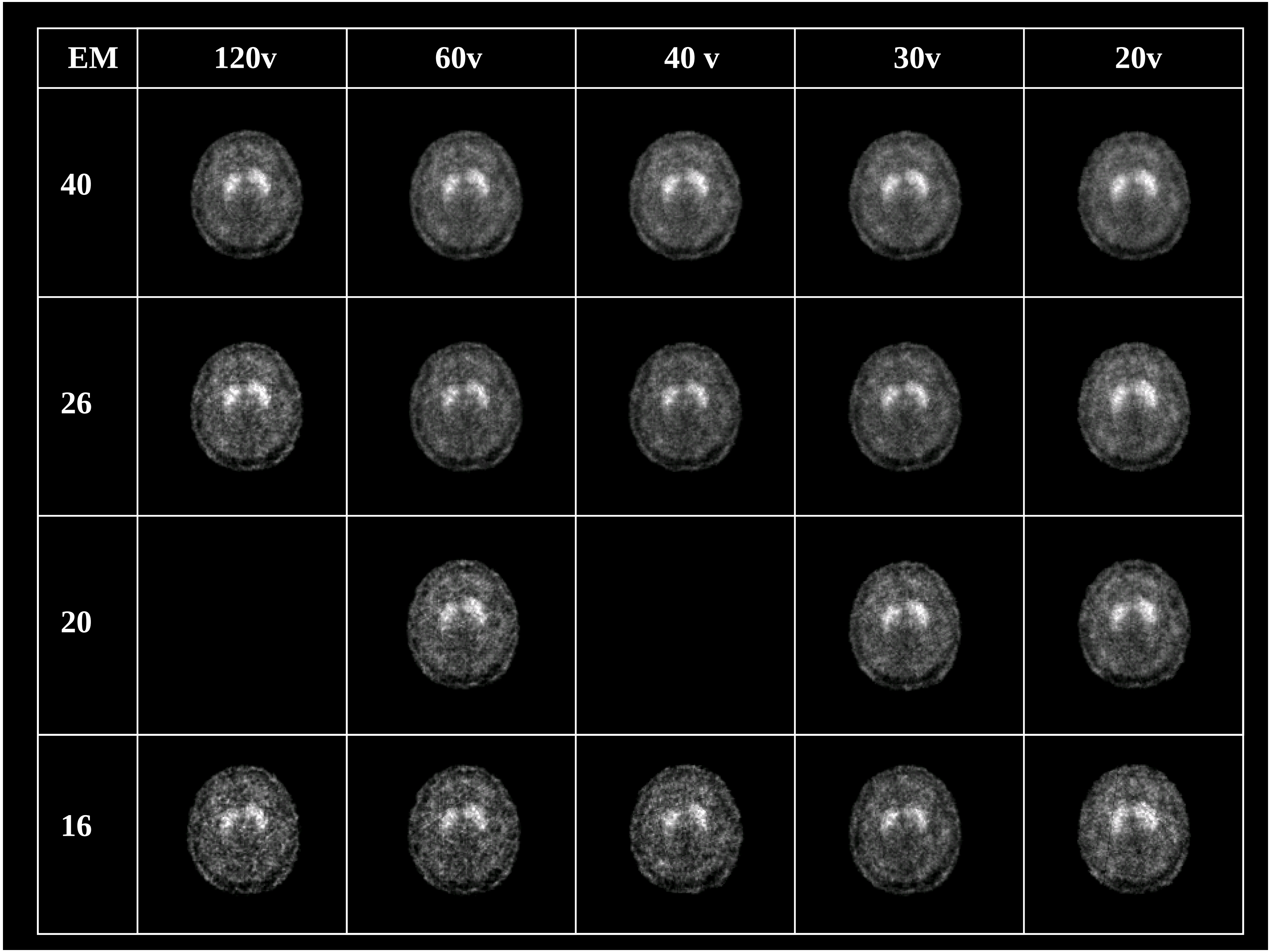
EM
120v
60v
40 v
30v
20v
40
26
20
16

Modeling of Edge Penetration in Pin-Hole SPECT (GATE)

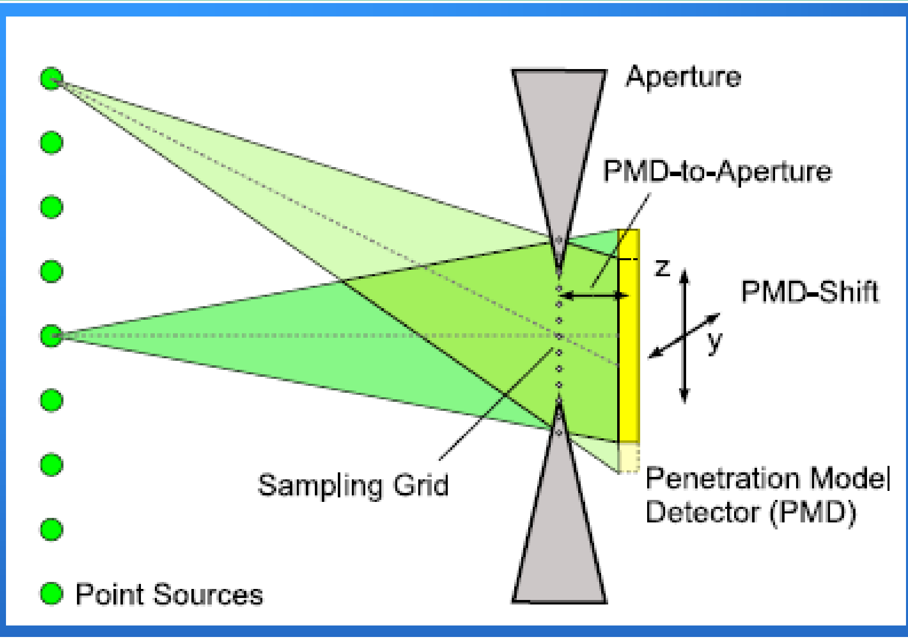

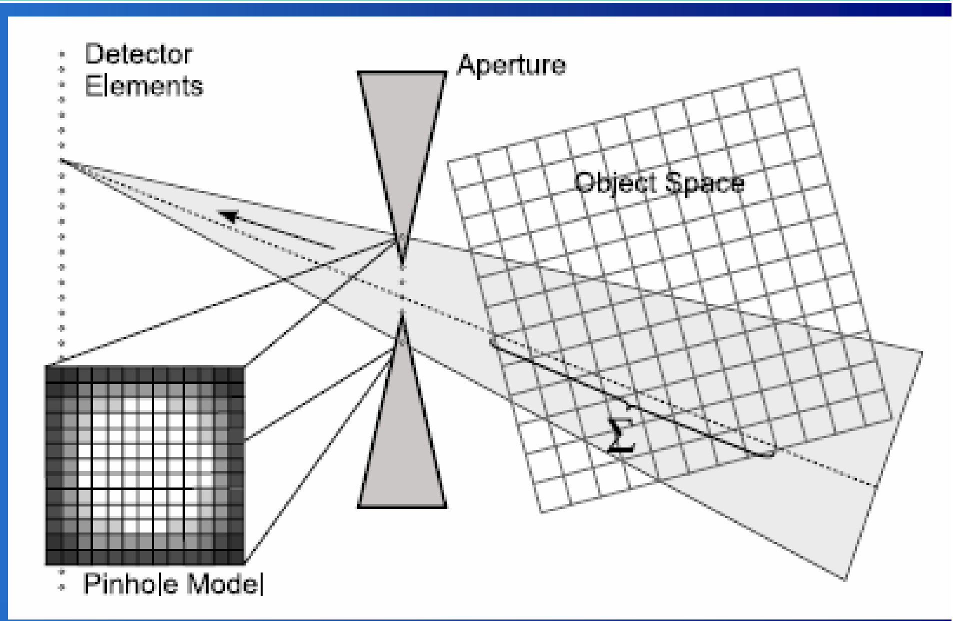

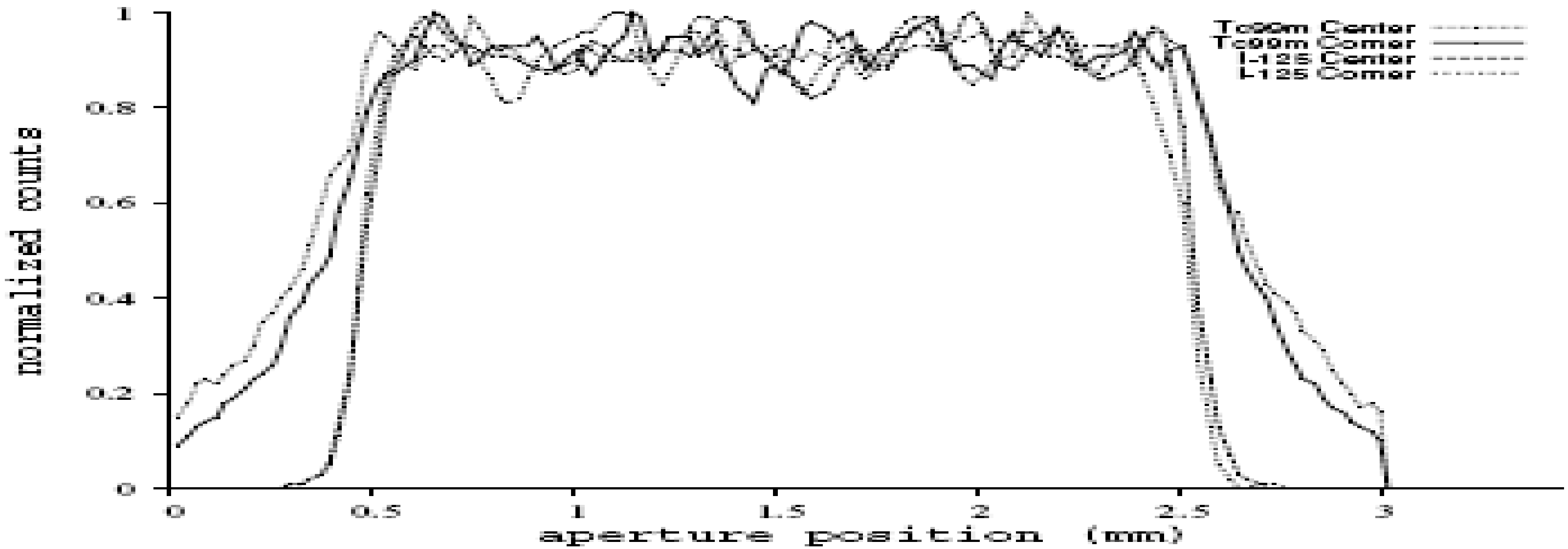

TOFPET DREAM

30 picosec TOF

4.5 mm LOR Resolution

10 picosec TOF

1.5 mm LOR Resolution

3 pico-sec TOF

0.45 mm LOR Resolution

Histogramming

No "Reconstruction"